Multiple Independent Extrusion Heads for Fused Deposition Modeling

John Paul Wachsmuth

Thesis submitted to the faculty of the Virginia Polytechnic Institute and State University
in partial fulfillment of the requirements for the degree of

Master of Science
in
Mechanical Engineering

Dr. Jan H. Bøhn, (Chair)
Dr. Donald G. Baird,
Dr. Robert H. Sturges, Jr.

February 1, 2008
Blacksburg, Virginia

Keywords: partition, parallel deposition, FDM, vector

Multiple Independent Extrusion Heads for Fused Deposition Modeling

John Paul Wachsmuth
Dr. Jan Helge Bøhn, (Chair)
Department of Mechanical Engineering

Abstract

Fused Deposition Modeling is a rapid prototyping technique in which miniature extruders melt filaments of polymeric materials. The extruder is mounted to an X/Y stage, and a computer controls the machine so that the polymer is deposited in only the appropriate locations. Material is deposited on one layer at a time so that the desired shape is built from the bottom up. While Fused Deposition Modeling has many advantages, it is poorly suited for large parts or for parts with thick walls due to the amount of time that is required to fabricate them. One strategy to reduce the build time is to implement multiple independent extrusion-heads. This thesis addresses various issues and concerns that arise while designing a multiple independent extrusion-head Fused Deposition Modeling system. The greatest design challenges and most critical issues are identified, and then solutions are presented. Physical samples and experiments verify feasibility when possible. Suitable material deposition strategies have been formulated to allow multiple independent extrusion heads to work simultaneously to reduce build time while allowing for a larger build envelope. These strategies produce parts that have nearly identical mechanical properties as those made on a single-head machine. This work seeks to provide information that is useful for designing a multiple independent extrusion-head Fused Deposition Modeling, regardless the number of extrusion heads or machine configuration. Implementing multiple independent extrusion heads will greatly reduce the fabrication time while allowing for a larger build envelope.

Acknowledgements

The author would like to thank the following people:

- Dr. Bøhn for allowing the use of his FDM machine to make samples, for providing a teaching position, and for being my advisor.
- Dr. Baird and Dr. Sturges for serving on my committee.
- Jamie Archual, Ben Poe, and Randy Smith for providing advice to repair the FDM machine.
- The staff at Asymtec, ERD, and Stratasys for helping diagnose the problems with the FDM machine.
- The Department of Mechanical Engineering machine shop staff for their help in building test fixtures and for lending me tools to use while working on the FDM machine.
- Dr. Molstad for sharing his humor and wit.
- Kanokwan Nontapot Wachsmuth for accepting an ABS ring fabricated by FDM with good humor (in lieu of one made from a precious metal).
- Mom & Dad for being understanding about the lack of repayment of the money borrowed during my undergraduate degree.
- Sanjay Kotha, Dr. Molstad, and Raffi Sahul for having confidence in me and for recommending me to the graduate school.

Table of Contents

Abstract ..... **ii**

Acknowledgements ..... **iii**

Table of Contents ..... **iv**

List of Figures ..... **vi**

List of Tables ..... **ix**

List of Tables ..... **ix**

Chapter 1
Introduction **1**
1.1 Rapid Prototyping 1
1.2 Motivation 8
1.3 Problem Statement 9
1.4 Solution Overview 10
1.5 Thesis Organization 10

Chapter 2
Literature Review **12**
2.1 Time Saving Concepts 12
2.2 Vector and Raster Graphics 15
2.3 Systems in Parallel or in Series 16
2.4 Observations 18

Chapter 3
Hardware **19**
3.1 Machine Design 19
3.1.1 Group Stages 21
3.1.2 The Minimum Separation Between Extrusion Heads 26
3.2 Calibration Issues 31
3.2.1 Planes of Motion and Z-Coordinate Calibration 32
3.2.2 Machine Coordinate System Calibration 37

Chapter 4
Software **40**
4.1 Toolpath Generation Overview 40
4.1.1 Terminology 42
4.1.2 Assumptions 44
4.2 Toolpath Generation 49

4.2.1 Perimeter Roads 51
4.2.2 Raster Roads 52
4.2.3 Seams 55
4.2.4 Toolpath generating algorithm 68

Chapter 5
Conclusions 91
5.1 Summary 91
5.2 Original Contributions 94

References 96

Curriculum Vitae 101

List of Figures

Figure 1 Illustration from Blanther's patent [Blanther 1892]. 2
Figure 2 (a) schematic of a LOM machine [eFunda 2005]. (b) part fabricated by LOM [PML Inc 2005]. 3
Figure 3 (a) schematic of SLA. (b) part fabricated via SLA [3D Systems 2005] 4
Figure 4 (a) 3DP system [MIT 2005]. (b) SLS machine [CERAM 2006] 5
Figure 5 Geometry containing an overhang starting at layer 5. 6
Figure 6 Schematic of a FDM [Cyon 2006]. 7
Figure 7 The interior of a fast build part being fabricated [ARC 2006]. 13
Figure 8 (a) The mechanical inner workings of an ordinary X/Y stage (cables, motors, and some pulleys are omitted for clarity). (b) A group stage would employ a longer Y-axis guide rod that would then be shared by two or more individual stages. 22
Figure 9 Front view of three adjacent X/Y stages. Stage 2 and stage 3's extrusion heads have been placed on a boom so their build volumes overlaps with the adjacent stages' build volumes. 23
Figure 10 Illustration of how pulleys can be arranged to produce overlapping ranges of motion on a group stage. 24
Figure 11 The tubes coming from the surrounded X/Y stage impedes the motion of another stage. 25
Figure 12 The group stages on the right are wider due to having individual stage that are wider than they are long. The length of the individual stages was reduced on the right so that the build volumes of the stages would not be increased. 25
Figure 13 A FDM with four extrusion heads, two next to each other and two across from each other. 27
Figure 14 Two identical extrusion heads facing one another. Dashed lines indicate the toolpaths of the extrusion heads when depositing roads from a particular type of nozzle (they could be either the build or support nozzles). (a) Case where the toolpath is at +45°. (b) Case where the toolpath is at -45°. 27
Figure 15 Case where extrusion heads that are mirror images are used. This time the minimum distance, D_m, is the same for (a) as it is for (b). 28
Figure 16 When identical extrusion heads are next to one another they will have the same minimum distance between them for both (a) +45° trajectories and (b) -45° trajectories. 29
Figure 17 A warped build due to the stages not being coplanar. 32
Figure 18 Illustration of a scheme for calibrating the Z coordinates of nozzles and making them coplanar. 34
Figure 19 Experimental rig at a 7° tilt. 35
Figure 20 (a) A test box to be made by two extrusion heads with dimensions L_0 and W_0. (b) The actual test box fabricated with dimensions L and W. 38
Figure 21 (a) The build volumes of four stages prior to MCS calibration. (b) The build volumes after calibration line up properly. 39
Figure 22 One layer of a rectangular part being fabricated by a FDM that has two extrusion heads. The color of the build-areas indicates which extrusion head

deposited the roads within them. The adjacent layers are mirror images of this one, so that the seam between roads deposited by different extrusion heads is reversed, accounting for the road-overlap areas. 43
Figure 23 Two parallel roads viewed through their cross section. 46
Figure 24 A microscopic image reveals a wide variety in the amount of fused area existing between two adjacent roads. Some roads share no fused area at all (outlined roads in the bottom layer), while others share a large amount (the outlined roads in the top layer share 66% of their thickness). The sample was fabricated on a FDM 1600 from ABS. The nozzle temperature was 270°C, the envelope temperature was 70°C, and the layers are 0.25mm thick. Standard Stratasys build procedures and default road spacing was used..... 46
Figure 25 Illustration of the possible alignment of polymer chains within two adjacent roads. 48
Figure 26 (a) Simple toolpath for a rectangular solid. (b) Complex toolpath for a solid containing a rectangular hole. 50
Figure 27 Photograph of a sample made with internal perimeters and an extra start/stop point in the perimeter. Note the fillets added by the FDM at the corners, which are sharp in the CAD model. The two adjacent fillets at the internal perimeters are visible by the naked eye at a distance of approximately 2 meters while the extra start/stop is only noticeable under close inspection. 52
Figure 28 (a) A 0°/90° raster. (b) A +/-45° raster. The color of the roads indicates which head deposited them. 54
Figure 29 (a) Cross section view of a part fabricated with a 0°/90° raster. The color of the roads indicates which head deposited them. Note the area containing many aligned fused regions where the roads change directions. 0° roads deposited by the second head transmit their stress through the fused region between the 90° roads deposited by the first head (white cross-section areas). (b) Cross section view of a part with a +/-45° raster. 55
Figure 30 Cross sectional view of a part made with a +/-45° raster with seams also alternating between +/-45°..... 56
Figure 31 (a) Two layers with seams that are located at the same location. (b) The case when the top layer is shifted to the left by an amount equal to the half the seam width. The displacement is in a direction perpendicular to the major axis of the overlap in X/Y stage motion. Note that the road-overlap area increases. (c) The case where the top layer is shifted parallel to the X/Y stage overlap by an amount equal to half the seam width. In this case the roads deposited by one head do not overlap with those deposited by the other head, and there is thus no road-overlap area..... 58
Figure 32 In the first case, the seam width was zero, resulting in no road overlap. The perimeter roads started and stopped at the seams (arrows). 61
Figure 33 In the second case, the seam width was 3.175 mm (0.125 inches), which is a quarter of the width of the tensile bar. This resulted in 20.2 mm^2 of road overlap area. The perimeter roads started and stopped at the seams (arrows). 61
Figure 34 In the third case, the seam width was 6.35 mm (0.25 inches), which is half of the width of the tensile bar. The third case had 40.3 mm^2 of road overlap area. Perimeter roads started and stopped at the seams (arrows). 62

Figure 35 In the fourth case, the seam width was 12.7 mm (0.5 inches), resulting in 80.6 mm^2 of road overlap area. The perimeter roads started and stopped at the seams (arrows). 62
Figure 36 In the fifth case, the seam width was 12.7 mm (0.5 inches) but was moved 14.3 mm from the center of the bar to create 443.6 mm^2 of road overlap area. The start/stop point of the perimeter roads are indicated by arrows. 63
Figure 37 The sixth case was the control and had no seam. It has 806.5 mm^2 of road overlap area, which is equal to the narrow section's length multiplied by the width. The start/stop point of the perimeter roads is indicated by arrows. 63
Figure 38 (a) Maximum tensile stress versus road-overlap area. (b) Maximum strain versus road-overlap area. Lines connect the average values, which are indicated by hollow squares. 65
Figure 39 Flow chart showing the process used to generate toolpaths. 69
Figure 40 (a) When the block is oriented with its length parallel to the long axis of the overlap in X/Y stage motion, then only one extrusion head can deposit roads at a time. (b) Rotating the part 90° allows both extrusion heads to work simultaneously. 71
Figure 41 Illustration of the grid used to count the area build by each head. When the part is at location 3, then the left head will deposit 15 squares of build material and 4 of support material. The right head will deposit 20 squares of build material and 48 of support material. 76
Figure 42 A multiple head FDM system with 2 stages in the X direction and 3 in the Y direction 79
Figure 43 Arbitrary shape built by a 6 extrusion head machine with 3 X/Y stages in a row. Each extrusion head has a first build-area in the X direction, a first build-area in the Y direction, and a second build-area. 82
Figure 44 Illustration of an arbitrary geometry that will have a first build-area far from the road-overlap area. 84
Figure 45 Toolpath generation using the highest-leftmost intersection for the start point. 86
Figure 46 (a) Simple toolpath resulting from the first build-area's width being an even multiple of the road width. (b) The complex case that arises when the width is an odd multiple of the road width. 87
Figure 47 The first build-area far from the road-overlap area (shaded green) is calculated for an arbitrary shape. The length of the toolpath is the same as the first build-area near the road overlap (shaded blue). The remaining second build-areas (shaded grey) also contain equal road lengths. 89

List of Tables

Table 1 Theoretical reductions in build time for various time saving techniques and combinations of techniques..... 14
Table 2 Approximate dimensions of extrusion heads on two different FDM systems.... 31
Table 3 The heights and angle between the stage and table before and after calibration. 35
Table 4 Summary of tensile data. 64
Table 5 Example of the areas calculated by counting rectangles in Figure 39. The highlighted values are stored in the matricies. Units = (road width)^2 77

Chapter 1

Introduction

An introductory understanding of Rapid Prototyping is presented here. This leads into a description of Fused Deposition Modeling (FDM) as well as some of its applications and limitations. Of particular concern are the limitations in part size and the insufficient build speed of the FDM to be used in some applications. Employing multiple independent extrusion heads is one solution to these problems. A brief overview of the challenges and difficulties in designing and building a multiple extrusion head machine is provided along with solutions to those issues.

1.1 Rapid Prototyping

The most general definition of rapid prototyping (RP) is any technology that allows prototypes to be created without the need for the time consuming fabrication of expensive tools (dies, stamps, etc.). Colloquially it is often used in reference to a technology that employs layered manufacturing to build up a prototype via the addition of materials as opposed to subtractive processes. Most machine shop tools (such as drills, lathes, end mills, and saws) would be considered subtractive processes because they remove material from bar, sheet, or rod stock until the desired geometry is all that is remaining. Additive processes, on the other hand, start with nothing and then through the deposition of material create the geometry. Typically this is done by depositing material one horizontal layer at a time only where needed, with each successive layer being stacked on top of the previous layer. An early example of such an additive process was used for the fabrication of three dimensional topological maps [Blanther 1892]. In this process sheets of wax were marked with the location of the topological map data and then cut out (Figure 1). When the sheets were stacked and bonded together, they created a scale replica of the

terrain. The leftover material that was removed was also stacked to make a negative of the terrain. After the edges were smoothed, paper could be placed between the positive and negative models and pressed to form a 3-D relief.

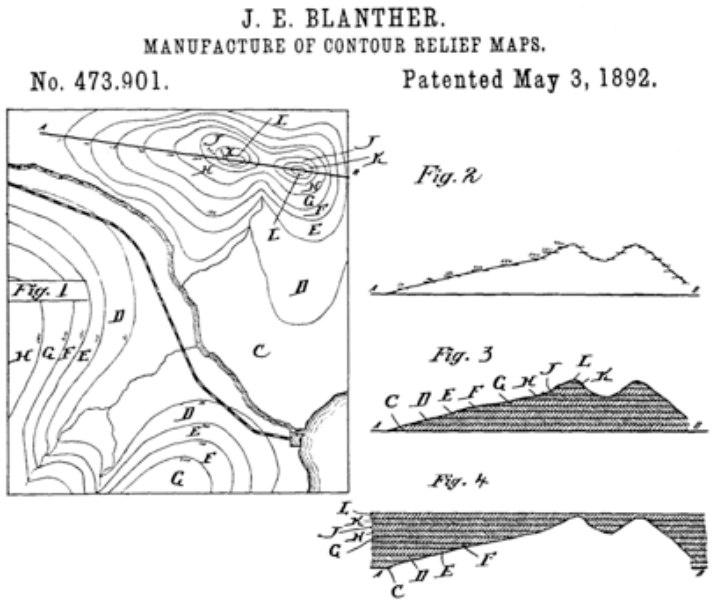

Figure 1 Illustration from Blanther's patent [Blanther 1892].

With the development of computers it became possible to automate the tedious process of placing material at the correct location of each layer while increasing the variety of usable materials and techniques. A process that is highly analogous to the one used for creating topological maps is Helisys Inc.'s Laminated Object Manufacturing (LOM). In this rapid prototyping machine (Figure 2.a), a CO_2 laser is used to cut paper or other sheet material in order to create the necessary material shape of each layer [Kai 1997]. The sheet begins on a roll on one side of the machine and then is bonded to the previous layer with an adhesive. The laser then cuts the shape out of the sheet in addition to cutting out a rectangular grid in most of the material that is not used, leaving only the edge of the sheet uncut. This grid allows the material that is not part of the desired geometry to be removed once the process is complete. The edge of the sheet is not

bonded to the previous layer, and is therefore free to be taken up by a second roller on the opposite side of the machine. As the leftover sheet is taken up it also advances the sheet so that new material is dispensed for the process to be repeated. After the process is complete the part is removed from the surrounding grid of blocks (Figure 2.b). Part fabricated by LOM have a finish that is similar to wood and can be machined. LOM is more suited for prototypes with thick walls because thin walls can be broken off while removing the build from the surrounding grid. Care must be taken to avoid building hollow parts as there is no way to remove the enclosed core once the build is complete. The paper that is vaporized by the laser raises fire and health concerns and therefore necessitates venting the fumes outside.

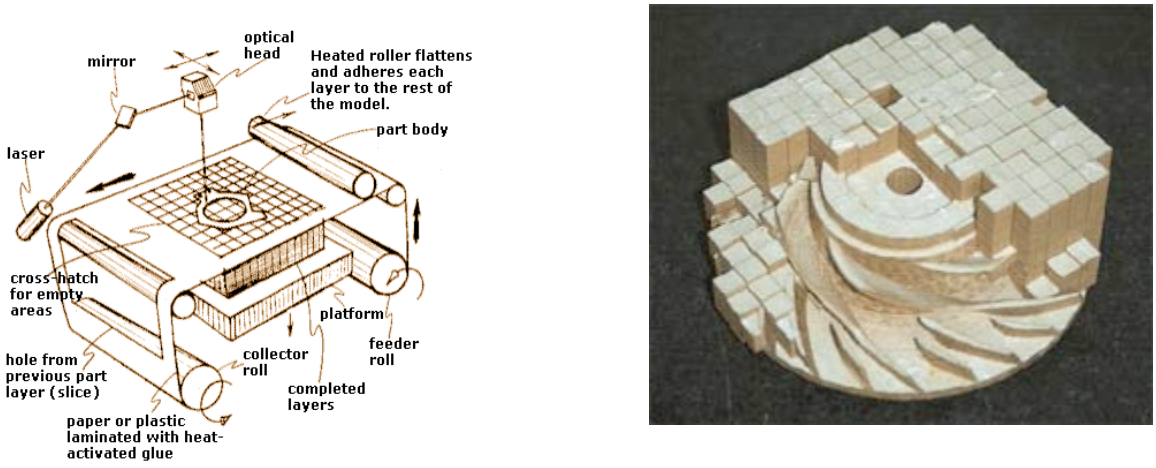

Figure 2 (a) schematic of a LOM machine [eFunda 2005]. (b) part fabricated by LOM [PML Inc 2005].

Not all additive rapid prototyping techniques take "layered manufacturing" as literally as LOM. Often times the layer to be added is itself built up over some period of time. One such RP system is 3D System's Stereo Lithography Apparatus (SLA). The SLA machine consists of a vat of liquid photoresist, a UV laser (Helium-Cadmium or

Argon ion), computer controlled optics to aim the laser, an elevator, and a wiper [Pham 2001].

Layered manufacturing with a SLA begins with the elevator initially positioned inside of the vat of photoresist so that a thin film of the liquid coats it (Figure 3.a). The laser then traces the desired geometry, causing polymerization of the monomer where solid material is desired. The elevator then lowers slightly and the wiper passes over the surface of the photoresist to smooth it out over the previously solidified layer. The process is repeated until the desired geometry has been solidified and then the elevator lifts the build up and out of the photoresist (Figure 3.b). The part is then drained, dried, and exposed to UV light for curing. While a Stereo Lithography Apparatus is capable of generating a superb surface finish, this advantage is offset by the relatively poor dimensional stability that results from the high creep rates of the polymer. Other disadvantages, such as the high cost and carcinogenic nature of the photoresist further limit the appeal of SLA.

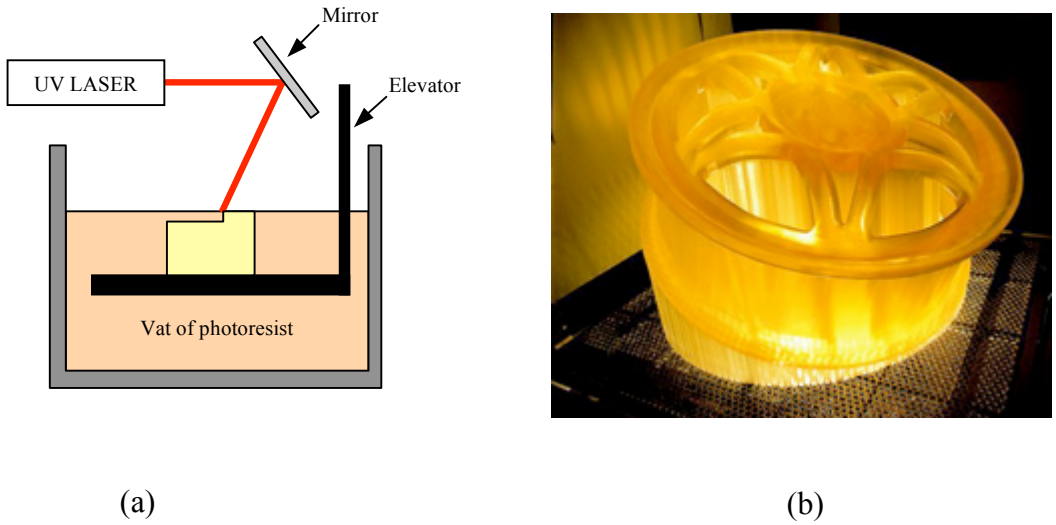

Figure 3 (a) schematic of SLA. (b) part fabricated via SLA [3D Systems 2005]

Some layered manufacturing systems employ powdered materials. Examples include Selective Laser Sintering (SLS) from 3D Systems Inc. and 3 Dimensional

Printing (3DP) developed at MIT and commercialized by Z Corporation. In both systems a thin layer of powder is spread over a piston [Noorani 2006]. 3DP employs ink jet printing technology to deposit a binder at locations where geometry is desired (Figure 4.a) while SLA uses a laser to loosely sinter polymer powder or polymer coated particles (Figure 4.b). In both cases the piston then lowers slightly and the next layer of powder is deposited. A counter-rotating drum is used to smooth and compact the powder and help control the layer thickness. The drawback of both systems is that the fabricated part is powdery and fragile. This necessitates additional infiltration and/or sintering steps. Also the elevated temperature within a SLS machine causes the bed of powder that surrounds the desired geometry to agglomerate and must therefore be discarded after being used only once. This contributes to both waste and cost.

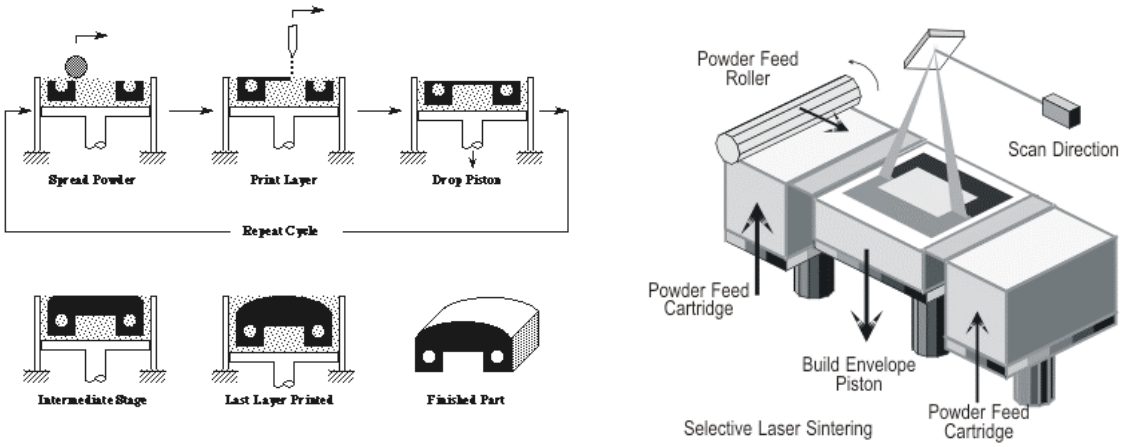

(a) (b)

Figure 4 (a) 3DP system [MIT 2005]. (b) SLS machine [CERAM 2006]

A slight complication occurs when the geometry to be fabricated contains an overhang – a piece of solid material that is not directly supported by the material below it. For example, suppose that a side view of the desired geometry looks like Figure 5. Everything goes just fine until layer 5, at which time the material on the right hand side is to be built in mid air! It is therefore important that layered manufacturing devices have a

strategy to deal with overhangs. In Laminated Object Manufacturing the overhanging material can rest on the grid of material below it. Likewise, in 3DP and SLS the bed of powder surrounding the previous layers' geometry can support the overhang (such a support is often referred to as an "intrinsic support"). In the Stereo Lithography Apparatus the overhang must be supported by solidifying a thin amount of material to the Z stage in the first four layers. This support material is then cut off with a knife and discarded after the part is removed from the vat. Due to the support being fabricated from the same material as the build material, it is sometimes difficult to tell them apart, much less to separate them.

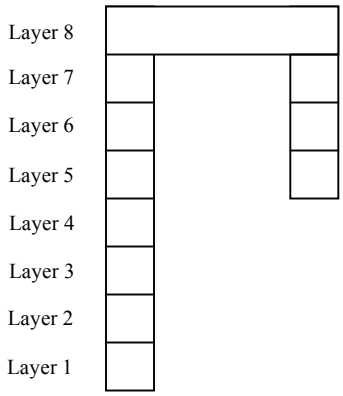

Figure 5 Geometry containing an overhang starting at layer 5.

One of the advantages of Fused Deposition Modeling (FDM) is the ease at which the support material can be identified and removed. A FDM machine consists of a Z stage, a chamber in which the temperature can be controlled, and two miniature extruders contained within an "extrusion head" that can be positioned by an X/Y stage (Figure 6). One extruder is used to lay down the build material while the other extruder lays down the support material. The support material is typically a different color than the build material so that they can be visually differentiated. This makes it easy to tell what is part of the desired geometry and what is a support structure. A slight chemical modification to the support material prevents it from bonding with the build material so that the

supports easily break away. Recently water-soluble support materials have become commercially available for very easy removal. As the extrusion head moves and deposits material, it leaves a trail of deposited material called a "road." The most commonly used materials are sold as thin filaments on spools and are polymers such as acrylonitrile butadiene styrene (ABS), nylon, wax, or elastomers. Fused Deposition Modeling can also deposit ceramic powders mixed with a binder [Griffin 2004] although an extrusion head capable of higher pressures may be necessary [Vaidyanathan 2000]. Metal parts can be fabricated using a metal/polymer composite as a filament. It is even possible to build metal/polymer composite tooling on a FDM using an appropriate polymer matrix [Masood 2005]. Parts made from ceramics or metals require an additional sintering/infiltration step. FDM has grown to become very popular due to its low cost, long lasting dimensional stability, wide range of materials, and safety. Out of all the commercially available rapid prototyping technologies, FDM is the only one not to involve hazardous fumes, carcinogenic chemicals, or messy powders. This has led to FDM being accepted as an "office friendly 3-D printer" that can be located in the same location as the designers who use it.

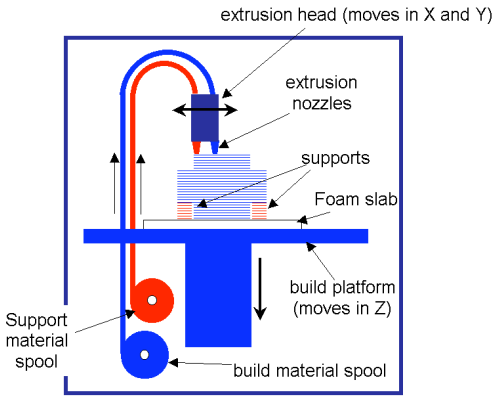

Figure 6 Schematic of a FDM [Cyon 2006].

While layered manufacturing techniques are often referred to as "rapid prototyping," a casual observer may note the relatively long time required for each build layer and the large number of layers required to form the desired geometry, and wonder if

this term is in fact a misnomer. Most RP systems require hours or even days to build a part, but this time is often shorter than the time required to machine the desired geometry using subtractive techniques, particularly in the case of thin walled, complex parts. Prototypes that would require injection molding to form are also much faster to fabricate using a RP system. This is because layered manufacturing techniques can build a part without the need to first machine tooling such as dies and punches. It can take weeks at a cost of tens of thousands of dollars to machine a die from tool steel, which is then difficult if not impossible to modify in the highly probable event that changes to the design are desired after evaluating the first few prototypes. Rapid prototyping, on the other hand, bypasses the need for tooling and therefore produces prototypes within hours, not weeks, and at a cost that saves tens of thousands of dollars. This is a particularly important advantage when several design/testing iterations are necessary to maximize the ergonomics or functionality of a component that is being designed.

1.2 Motivation

In the literature many authors have commented on the positive effect that rapid prototyping has had on manufacturing and product development [Beaman 1997; Jacobs 1996; Kai 1997; Kamrani 2006; Noorani 2006; Pham 2001]. Two schemes for employing a RP system to enhance traditional manufacturing are typically discussed, both of which are commonly referred to as "rapid manufacturing" (RM). The first method is to use a RP machine to fabricate the tools needed for manufacturing, a scheme that is often called "rapid tooling" [Bennett 1995; Hilton 2000; Pham 2001]. Alternatively, the RP machine could be used to do away with tooling altogether and directly manufacture a product without any tooling [Hopkinson 2006; Kamrani 2006; Lind 2003]. This is highly attractive when only a very small production run is desired or the product would need to be customized. However, the current state-of-the-art FDM machine is insufficient for manufacturing large parts quickly. It has been speculated that an increase in build speed of two or three orders of magnitude would be required for

FDM to be practical for the tool-less manufacture of ceramic components [Halloran 1999].

There also exists a limit in the size of the build envelope that is practical with FDM machines. This limit is largely caused by the increase in build time required to fabricate larger forms. A larger build envelope results in the extrusion head needing to travel a longer distance in order to lay down all the roads. This in turn increases the amount of time necessary for each build layer to the point that it is not practical to significantly increase the build envelope beyond its size in current FDM machines. An additional factor is that larger X/Y stages require larger moving parts (the wires, guide rods that the head moves on, tubes that connect to the extrusion head, etc.). The added mass reduces the maximum acceleration, and therefore slows the motion of the extrusion head.

Multiple independent extrusion heads could be used to increase the build envelope without significantly increasing the build time. This could in effect allow an object to be fabricated that is several times the size of the current build envelope without increasing the amount of fabrication time that is required. Using multiple extrusion heads is also a new strategy that could be implemented in addition to other time saving schemes to create the fastest possible FDM for tool-less manufacturing purposes. The implementation of multiple extrusion heads would therefore greatly aid in the practicality of employing FDM for both the fabrication of rapid tooling and tool-less manufacturing. The design of an FDM machine that employs multiple independent extrusion heads with limited overlap of build volume will therefore be considered here.

1.3 Problem Statement

The amount of time required to fabricate large parts limits the size of the build envelope as well as the acceptance of FDM in RT and RM applications. There therefore exists a

need for a new scheme that can be implemented to reduce the required build time of large parts. Ideally, this new scheme should be compatible with existing schemes so that the greatest total time savings can be achieved by implementing multiple time saving schemes at once.

1.4 Solution Overview

One possible time saving scheme is to employ multiple independent extrusion-heads. Each extrusion head would have its own X/Y stage and would therefore be capable of moving independently. The part to be fabricated would then be partitioned into regions lying within the ranges of motion of the different extrusion heads. A common Z stage would be utilized so that concurrent deposition by the heads is possible. The ranges of motion of adjacent extrusion heads should overlap some so that the roads that are deposited by one head can overlap with the roads deposited by the other head on adjacent layers. This overlap assists in fabricating acceptably strong parts. With an appropriate road deposition scheme the extrusion heads will be capable of simultaneous motion so that they cooperatively deposit the roads needed to fabricate a part. This will significantly reduce the amount of time that is required.

1.5 Thesis Organization

This work is organized into five chapters. Experiments are presented at appropriate points in the text so that a cohesive dialog is presented. An outline of this work is as follows:

Chapter 1 presents introductory information pertaining to rapid prototyping, particularly FDM. The motivation for building a multiple independent extrusion head FDM machine is explained, followed by the problem statement and solution overview.

Chapter 2 is the literature review. It starts with an examination of other investigators' work in developing strategies to reduce the required fabrication time to fabricate a part via FDM. It then attempts to draw parallels between computer graphics and RP systems. Parallel processes are discussed and then observations are made about the relevant literature.

Chapter 3 addresses the hardware issues that arise in a multiple independent extrusion head FDM machine. As such, it begins with an overview of the design of a multiple extrusion-head machine that is presented in this work. This leads into a discussion of how multiple X/Y stages can be combined to reduce the amount of required calibration and to facilitate creating overlapping build volumes. The minimum separation between extrusion heads to prevent a collision is then examined as a function of geometry and the physical dimensions of the heads. Chapter 3 concludes by addressing the calibration issues that arise due to the need for the roads deposited by different extrusion heads to align were they meet and to be coplanar so that the fabricated part is not warped.

Chapter 4 is concerned with software issues, particularly the development of a toolpath generating algorithm. Emphasis is placed on avoiding a collision between the extrusion heads, fabricating mechanically strong parts, and minimizing the required build time. Once deposition of the perimeter and raster roads are discussed, empirical data is used to correlate the strength of the fabricated part to the amount of overlap between roads deposited by different extrusion heads on adjacent layers. An algorithm is also presented to optimize the position of the part within the build time for the greatest time savings.

Chapter 5 is the last chapter and contains the conclusions. It also summarizes chapters three and four.

Chapter 2

Literature Review

This work is concerned with increasing the fabrication speed and build volume of Fused Deposition Modeling. The literature review will therefore start with a brief exploration of several time saving strategies that have been developed specifically for FDM. It will then draw parallels between computer graphics and RP systems before discussing systems that are in parallel or in series. The chapter concludes with observations about the relevant literature.

2.1 Time Saving Concepts

There are several software and hardware concepts that can be implemented to reduce the time needed to fabricate a part via FDM. One example is local adaptive slicing, in which software analyzes the slope of the walls of individual features. The FDM is then directed to use thick build layers for areas with near-vertical walls and thin layers for near-horizontal surfaces. This results in thick build layers being used whenever it does not sacrifice surface quality. Due to needing fewer build layers, local adaptive slicing can save about 55% of the build time [Tyberg 1998]. Another technique is to use thin build layers for the outer surface to retain a high quality surface and a thick fill raster to quickly fill interior volumes. For thick walled parts, this can save 50-80% of the time needed to build a part [Sabourin 1997]. Commonly suggested hardware improvements include increasing the movement acceleration and maximum velocity of the X/Y stage. A hypothetical increase of 30% would correspondingly reduce the build time by about 30% (the actual reduction in build time is likely to be slightly less due to time that the extrusion head is stationary or slowly moving, such as beginning or terminating a road).

Designers occasionally wish to fabricate a prototype for the purpose of design verification or aesthetic evaluation as quickly as possible without concern for the mechanical strength of the part. The software provided by Stratasys to control FDM machines has addressed this need by allowing the operator to instruct the FDM to fabricate a "fast build" part using a sparse internal structure [Stratasys 1997]. In a fast build part, the FDM deposits raster roads in a cross hatch or honeycomb pattern that incorporates some empty space between the roads (Figure 7). This necessitates depositing fewer roads and therefore reduces the required build time.

Figure 7 The interior of a fast build part being fabricated [ARC 2006].

While applying the various time saving techniques that have been developed for FDM will greatly increase the speed at which a part can be fabricated, these improvements most likely cannot account for more than a 4-fold increase in build speed. This is because the time savings from local adaptive slicing is due to using the thickest layers possible, resulting in a thick raster fill being used more often. Employing thick raster fills all the time would therefore only offer additional time savings when thin build layers are used *and* the geometry permits a thick internal raster. The resulting total time savings of combining local adaptive slicing with thick fill raster will therefore be highly dependent on the geometry being fabricated; a reasonable estimate would be a 60% reduction in build time. When combined with the 30% hypothetical build time reduction achievable through hardware improvements, the total time savings would be 72% (a 3.6

fold improvement). Table 1 lists the approximate reductions in build times when various time saving techniques and combinations of time saving techniques are implemented. In order to further reduce build times, additional methods of increasing build speed are needed. New methods should be capable of being implemented concurrently along with the changes to the FDM that are suggested above to achieve the maximum benefit. One possibility is to implement multiple independent extrusion heads. This would allow the build envelope to be subdivided, with each extrusion head simultaneously building a section of the part, therefore reducing the total build time.

Table 1 Theoretical reductions in build time for various time saving techniques and combinations of techniques.

Time saving technique	Theoretical reduction in build time
local adaptive slicing	approximately 55% (when multiple features or parts are present, each with a different ideal layer thickness)
thick fill raster	50-80% (for thick walled parts)
hardware improvements	30% (hypothetical)
local adaptive slicing combined with thick fill raster	approximately 60%
local adaptive slicing, thick fill raster, and hardware improvements	approximately 72%

Despite the potential of a multiple extrusion head FDM, only one example could be found in literature. Zhu and Yu explored a two head system where the extrusion heads had entirely overlapping ranges of motion for the purpose of building a composite structure from two materials or colors [Zhu 2002]. A summary of their scheme is as follows. Each build layer is first divided into regions to be filled by the different materials. Toolpaths are generated for each individual region without attempting to determine the order that they will be filled. A spatio-temporal model is then applied to each region to predict the locations of the extrusion head while filling that region. In a spatio-temporal model, time is treated as another spatial dimension. The 2-D foot print of an extrusion head is therefore extruded into a 3-D solid, with the third dimension

representing time. This has the drawback of requiring precise knowledge of the position, velocity, and acceleration of the extrusion head for all times that it is filling a region. Collisions between extrusion heads are represented as interferences in the 3-D solids. Regions can then be placed into groups that can be deposited without a collision. Once one head has completed its region, it will wait for the other head to finish before they both begin filling regions in the next group (provided that another collision free group exists). Regions that cannot be placed into a collision free group are deposited one at a time while the other extrusion head waits. Because one extrusion head will be required to wait while the other head completes its region or when there is not a collision free pair of regions, Zhu and Yu's scheme will only produce limited time savings. However, this is not a major detraction because their work is concerned with producing multi-material parts, and any time savings can be considered as an added benefit.

Zhu and Yu's work and the work presented in this thesis differ significantly in four ways. First, their work was concerned with the fabrication of a multi-material part whereas in this thesis the emphasis is placed on reducing the build time for large parts. Secondly, the construction and design of the physical machine will be considered in this thesis in addition to software concerns. Zhu and Yu only considered software. Thirdly, the machine proposed by Zhu and Yu had extrusion heads with entirely overlapping ranges of motion. In this thesis only limited overlaps in the ranges of motion will occur so that the build envelope can be as large as possible. This prevents cases where one region surrounds another. Finally, as a result of the separation of build regions, the control scheme that is proposed in this thesis will generally be less computationally expensive and easier to implement than a spatio-temporal based scheme.

2.2 Vector and Raster Graphics

Analogies can be drawn between various RP systems and computer graphics. In computer graphics, images can be represented by vectors or as a raster format. Vector

representations use mathematical equations to describe primitives (such as lines and curves) whereas raster images describe the color and intensity of individual pixels [McMahon 1998]. Vector representations have the advantages of requiring less memory and of retaining detail when enlarged. Raster images have the advantage of being capable of displaying textures. All modern computer displays translate vector representations into raster representations that are then used to instruct the monitor how to illuminate each pixel [Wikipedia 2006]. However, CRTs that were used with early computer systems traced out lines and curves onto a phosphorescent screen using a beam of electrons. Those monitors were therefore vector based, whereas modern displays are raster based.

If we define a vector system as one that specifies lines and arcs and a raster system as one that specifies points in a matrix, then many devices can be classified as vector or raster systems. For example, 3DP would be classified as a raster system as it sprays binder only at the necessary points. FDM could be considered as a vector system since the X/Y stage moves the extrusion head along lines and curves while it deposits a stream of polymer. Other examples of vector systems in RP are LOM, SLA, and SLS.

2.3 Systems in Parallel or in Series

The approach that is presented in this thesis has more in common with parallel processing than with most previous efforts in the RP field due to partitioning the part to be fabricated into areas that will be deposited by different extrusion heads. In parallel processing an array of processors is matched to an array of memory elements, data, or instructions [Fountaim 1994]. This allows a complicated computational task to be essentially subdivided amongst several processors so that they each perform a fraction of the task concurrently. Parallel processing thus greatly reduces the time required for accomplishing such a task, resulting in its use in virtual simulations, data mining, and transaction processing [Grama 2003]. Poor load balancing, synchronization overheads,

and memory access conflicts can reduce the efficiency of parallel processing [Kontoghiorghes 2006]. Similarly, the efficiency of a multiple independent extrusion-head FDM will be decreased if one extrusion head is forced to wait while another one deposits roads, while the Z stage is actuated, or in order to avoid a collision. Emphasis will therefore be placed on allowing simultaneous movement of all extrusion heads so that the greatest time savings are realized.

Almost any task that is performed by a single device can be completed at a higher rate by employing multiple devices. In general there are two distinct methods by which to do this. The first method is to place the devices in parallel and then have them work independently. For example, if one device is capable of producing n units per second, placing another identical device next to the first one would allow for a theoretical production rate of $2n$ units per second. This optimum production rate will not be realized unless work can be supplied to each device at the original (single device) rate, the products removed from each device at a sufficiently high rate to prevent accumulation, and the two devices are capable of operating at the same time. An example of a parallel processes is the case where two identical manufacturing lines are used to produce twice the number of parts that a single line could handle. The second method by which devices can work together is to place them in series and then have them work cooperatively on the same task. In this case the work is divided between the devices, with each one doing an equal fraction of each task. Obtaining the optimum production rate requires the same criteria as in the first case in addition to the need to divide each task evenly between the devices. Otherwise at least one device will idle inefficiently while waiting for the last device to finish its part of the task before the devices can move on to the next task. An example of a system of devices in series is the pit crew that changes the tires on a race car. One crew member may be capable of changing the tires in n seconds while four crew members can change them in $n/4$ seconds. However, if three crew members worked together, then one person will have to change two tires and the required time will be equal to the time that the overburdened crew member requires: $n/2$ seconds.

Raster systems can be considered to be comprised of many point sources that have been arranged to be in parallel. Increasing the potential for a raster system to do work (often measured in terms of size) becomes a matter of increasing the number of pixels, spray nozzles, etc. Vector systems, on the other hand, can be placed in either parallel or in series. A multiple extrusion head FDM machine can be constructed from several X/Y stages, each with its own extrusion head. When multiple small parts are fabricated by the machine, the parts can be arranged within the build volume such that each extrusion head fabricates the same number of parts. During this type of usage the extrusion heads are placed in a parallel arrangement. The extrusion heads behave as though they are in series when the machine is used to fabricate a single, large part by subdividing the part into regions that lie within the ranges of motion of the different extrusion heads.

2.4 Observations

The relevant literature implies the following observations about a multiple extrusion head FDM system:

1) Although many strategies exist to reduce the amount of time required by FDM to fabricate a part, little work has been done towards employing multiple extrusion heads for the purpose of reducing build time.
2) FDM can be thought of as being similar to vector based computer graphics in that the X/Y stage moves the extrusion head along lines and curves. Other RP systems may be similar to raster graphics systems.
3) Increasing the number of devices working on a task can increase the rate of completed tasks per unit time. This can be achieved by placing the devices in either parallel or in series. In both cases it is important that the devices are capable of operating concurrently without interfering with each other. Maximum time savings are realized when all the devices operate simultaneously. This in turn places importance in subdividing the task equally amongst the devices.

Chapter 3

Hardware

This chapter begins by providing the reader with an overview of the proposed design of a multiple extrusion-head FDM machine. Assumptions about the machine are stated, and the maximum possible number of extrusion heads is examined. An explanation is then provided about how several individual X/Y stages can be combined into a single "group stage" that reduces calibration at the same time as it provides a mechanism for creating overlapping ranges of motion between the stages. The minimum separation that must be maintained between the extrusion heads is then shown to be a function of the dimensions of the head and geometry. With the general machine design specified, the additional calibration issues that arise for a multiple extrusion-head FDM machine are examined. These calibration issues include the planes of motion and Z-coordinates of the nozzles, and the machine coordinate systems of the X/Y stages.

3.1 Machine Design

Calibration and software issues will arise that are specific to the design of a multiple-extrusion head FDM machine. It is therefore worth examining the general design of a multi-head machine that will be considered in this thesis prior to proceeding to the other issues. In this thesis a multiple extrusion-head FDM machine will have more than one extrusion head, and each head will be assumed to be identical. Furthermore, the heads will be assumed to be unmodified, except for having an additional solenoid on the build nozzle. Commercially available extrusion heads have a solenoid on the support nozzle so that it can be lifted out of the way when it is not depositing material. The additional solenoid on the build nozzle will allow it to be lifted up to allow roads to be terminated without moving the Z stage and to allow it to clear previously deposited roads. With the

extrusion heads otherwise unmodified, they will be approximately rectangular in shape and will be connected to a stationary point on the FDM machine via tubes that contain the electrical wires, filament strands, and allow for cool air circulation. Each extrusion head will be suspended from its own gantry type X/Y stage so that the heads can be moved independently of one another. The stages will be placed next to each other in a rectangular array and will have a limited amount of overlap in motion. In the next chapter it will be explained how the overlap will assist in optimizing the fabrication time by allowing the boundary between roads deposited by different extrusion heads to be shifted, thereby assisting in equalizing the amount of time that each extrusion head requires. The overlap will also be shown to increase the mechanical strength of fabricated parts by allowing the roads deposited by one head to overlap with roads deposited by the other head on adjacent layers. The X/Y stages will be computer controlled and the nozzles of all extrusion heads will be coplanar so that a single, common Z stage can be used. The Z stage will have at least as much length and width as the combined build volume of all the X/Y stages.

As stated above, it is simply assumed that the multiple extrusion-head FDM machine will have more than one extrusion head. The reason why a particular number of heads is not specified is because different applications may require a different number of extrusion heads. For example, two X/Y stages would likely be employed for tool-less manufacture as most components are small enough to fit within the combined build envelopes. This is because most items of interest for tool-less manufacture are to be customized to match the physical traits of a human being or are products that will be handled by a person. Examples include customized medical products (such as bone grafts [Chen 2004], chin implants [Singare 2005], tooth crowns [Wang 2004], and pre-surgical planning aids [da Rosa 2004]), products that need to conform to an individual's unique shape (such as custom fit radiotherapy masks [de Beer 2005] and aircrew oxygen masks [Elkins 1997]), consumer products with a very limited production run, pilot production runs, and volume beta testing [Elliott 2004]. The primary benefit from employing multiple extrusion heads in a FDM machine designed for tool-less manufacturing is therefore the reduced fabrication time, not the increased build volume.

Alternatively, more than two X/Y stages may be desired for building large items that cannot fit into the current FDM build envelope. This includes tooling as well as large prototypes such as those that may be encountered when designing automotive, aerospace, and nautical components.

3.1.1 Group Stages

A multiple extrusion-head FDM machine with many X/Y stages would require a large amount of calibration. A reduction in the calibration that is required could be realized by combining two or more X/Y stages by employing shared guide rods. Such a X/Y stage will hereafter be referred to as a "group stage". In order to understand this concept, it is important to first understand the functioning of an X/Y stage. A stage has a high precision guide rod on each side that runs the length of the stage (Figure 8.a). A Y-axis carriage on each rod is pulled along by a system of pulleys and wires. Two X-axis guide rods link the Y-axis carriages and support the X-axis carriage, which is moved in the X-direction by another system of pulleys and wires. The FDM extrusion head is suspended on the X-axis carriage and, through the motion of the X and Y-axis carriages, can be positioned at a particular coordinate. It is possible to instead use Y-axis guide rods that are twice as long as in a normal X/Y stage and then place two sets of carriages and X-axis guide rods on them (Figure 8.b). This results in a group stage that incorporates two X/Y stages, although in theory any number of smaller X/Y stages could be combined into a single group stage by using long enough Y-axis guide rods. Group stages have the important advantage of being coplanar after the Z-coordinates of the nozzles are calibrated.

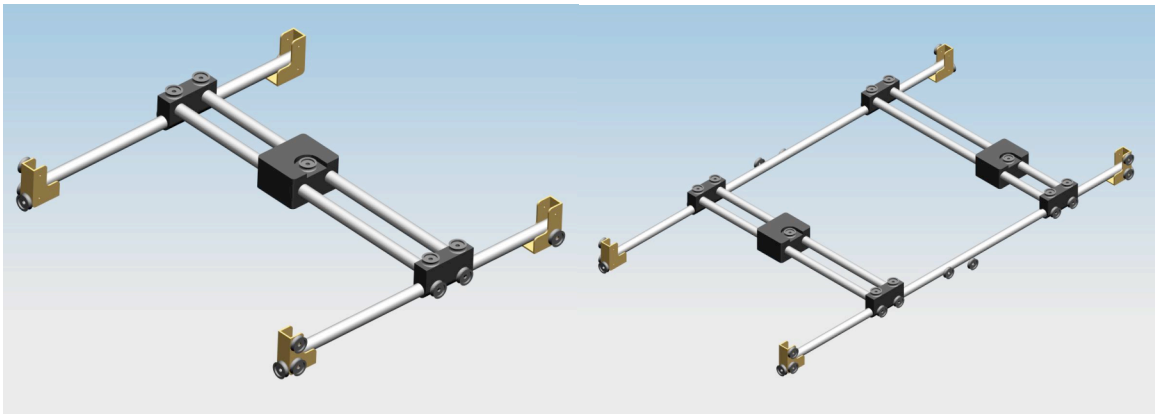

(a) (b)

Figure 8 (a) The mechanical inner workings of an ordinary X/Y stage (cables, motors, and some pulleys are omitted for clarity). (b) A group stage would employ a longer Y-axis guide rod that would then be shared by two or more individual stages.

Group stages also have another important advantage: they are capable of being designed to allow for overlapping ranges of motion between the stages. For a multiple extrusion head FDM to fabricate a part, it is important that the roads deposited by one head can slightly overlap with the roads on adjacent layers that were deposited by the other head. This road overlap is planned during the partitioning of the build and will be shown in the next chapter to increase the mechanical strength of the part where the areas deposited by different extrusion heads meet.

When two X/Y stages are used, it is possible to create overlap in the build volumes by placing one or both of the stages on a boom so that it hangs several centimeters farther towards the other stage than the location of the X-axis carriage. However, this becomes impractical for a large number of stages because each consecutive stage must be placed on a progressively larger boom to reach the adjacent build volume (Figure 9). The increasing length is needed in order to compensate for the difference between the width of the X/Y stage and its build volume. Telescoping booms could be used, but telescoping booms would add cost, complexity, and considerable mass

due to needing to be highly rigid. The tremendous increase in the mass of the extrusion head would greatly reduce the acceleration of the X/Y stage, slowing the fabrication rate. Group stages can overcome this problem in the Y direction at least, by placing the pulleys such that the Y-axis carriage of the first stage can be pulled past the pulley for the Y-axis carriage of the second stage (Figure 10). Making one set of pulleys higher than the other will prevent the wires from touching. This can be easily recognized by examining the equation that describes the plane swept out by a wire as the stage is actuated:

$$aX + bY + cZ + d = 0 \qquad \text{Equation 1}$$

Increasing the height of the pulleys on the carriage and attaching them to the frame increases the value of the parameter *d* without modifying any other parameter. As a result, the planes swept out by the two wires are parallel but offset by an amount equal to the difference in pulley heights. The wires are thus incapable of physically touching. The extrusion heads, on the other hand, are capable of colliding. The heads must therefore be separated by at least the minimal distance to prevent a collision. This minimal distance will be shown in the next section to be a function of geometry and the size of the extrusion head.

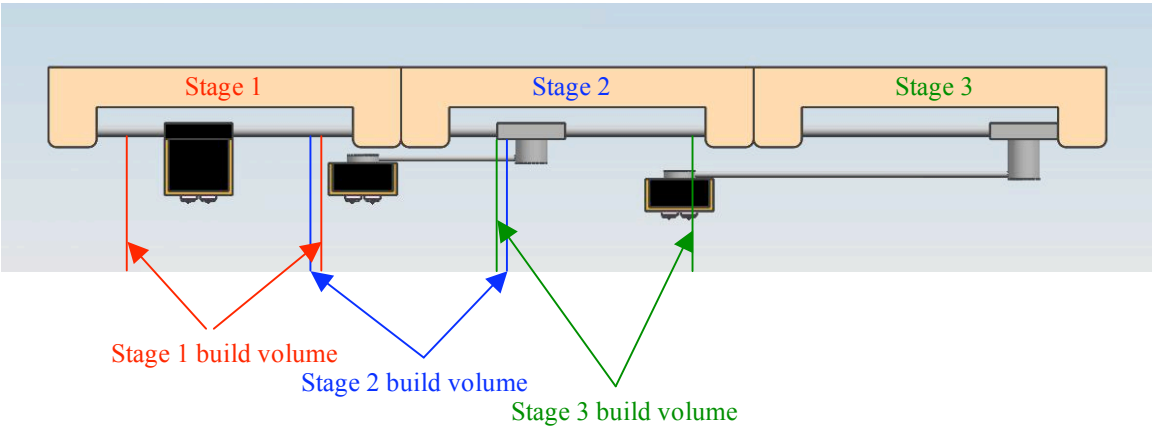

Figure 9 Front view of three adjacent X/Y stages. Stage 2 and stage 3's extrusion heads have been placed on a boom so their build volumes overlaps with the adjacent stages' build volumes.

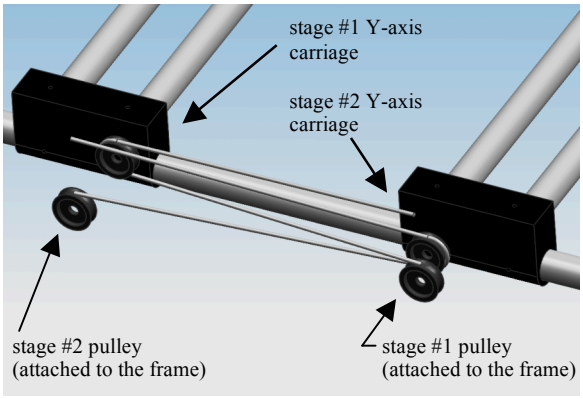

Figure 10 Illustration of how pulleys can be arranged to produce overlapping ranges of motion on a group stage.

While the shared Y-axis guide rods of a group stage allow any number of stages to be placed next to each other, not more than two stages will usually be positioned across from each other. Part of the reason for this is the need for booms of rapidly increasing length to achieve overlapping ranges of motion as previously explained. The other reason is that when a stage is surrounded on all sides by other stages, there is nowhere for the tubes that connect to the surrounded extrusion head to go without inhibiting the motion of some other stage (Figure 11). Significant redesigns of the extrusion heads and X/Y stages may allow the tubes to be positioned vertically so that they do not interfere with each other. However, this would greatly increase the cost and complexity of the X/Y stages, which contain many horizontally positioned wires that would have to be somehow repositioned to prevent a collision with the vertical tubes. A simpler solution is to use stages that are wider than they are long so that the build volume of each stage is the same but the group stage is wider (Figure 12).

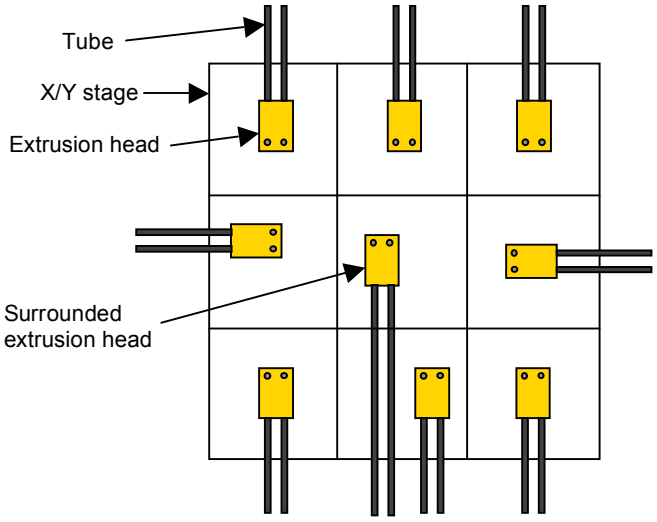

Figure 11 The tubes coming from the surrounded X/Y stage impedes the motion of another stage.

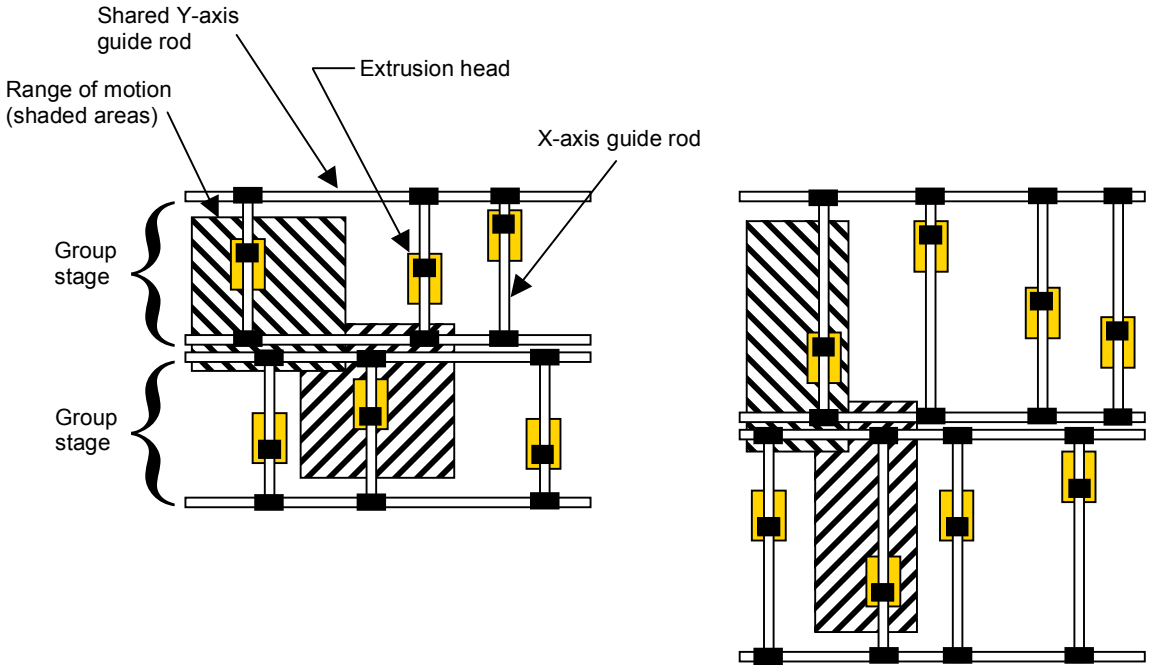

Figure 12 The group stages on the right are wider due to having individual stage that are wider than they are long. The length of the individual stages was reduced on the right so that the build volumes of the stages would not be increased.

3.1.2 The Minimum Separation Between Extrusion Heads

Extrusion heads must be separated by some distance so that they do not collide. As will be shown in this section, the minimum separation limits the smallest part that can be fabricated by more than one extrusion head depositing roads concurrently. It is therefore advantageous to have the smallest possible separation between extrusion heads. The required amount of separation is a function of the size, shape, and layout of the extrusion heads. It will be assumed here that the extrusion heads are rectangular with one build nozzle and one support nozzle (a slight adaptation may need to be made for extrusion heads with different shapes or that include a third nozzle for wide raster fills). Depending on the configuration of the multiple independent extrusion-head FDM, extrusion heads may be next to one another or across from one another (Figure 13). In either case the extrusion heads follow +/-45° trajectories while depositing raster fill roads. When identical extrusion heads are positioned opposite one another, they will be closest together when the upper corner of one head is near the lower corner of the other head. From this location, straight line trajectories that are parallel will not bring the extrusion heads any closer together. From geometry and the shape of the extrusion heads, it is then possible to find the minimum distance (D_m) between the toolpaths of the extrusion heads:

$$D_m = x + y * \tan(\theta) \qquad \text{Equation 2}$$

where x is the horizontal distance between nozzles of the same type (i.e., build or support material), y is the vertical separation between them, and θ is the angle made between the horizontal direction and the path that the extrusion heads will follow. Because the raster roads are at +45° or -45°, the tangent term equals one and the minimum distance simply equals the sum of x and y. It can be shown that identical extrusion heads situated across from one another will have two different minimum separation distances, depending on if the nozzles are close to each other or far apart from each other, which in turn depends on the angle of the toolpath (Figure 14). This is no cause for undue concern, as the larger of the two minimum separation distances should be used in such a case. A superior strategy is to make the extrusion heads mirror images of one another by switching the build and

support nozzles on one extrusion head. This results in a minimum separation distance that is the same for both +45° and -45° trajectories (Figure 15). The separation is the average of the two different separations found in the case where identical extrusion heads are utilized. As such, the minimum separation distance will be less when extrusion heads that are mirror opposites are used.

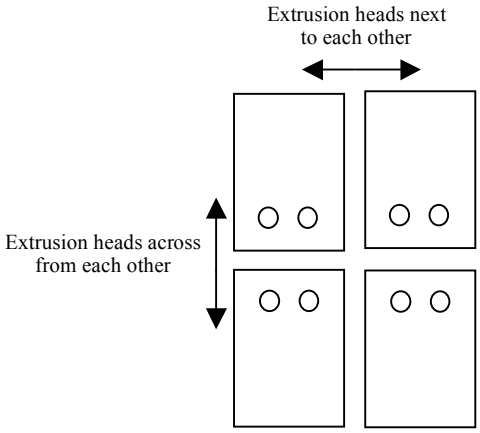

Figure 13 A FDM with four extrusion heads, two next to each other and two across from each other.

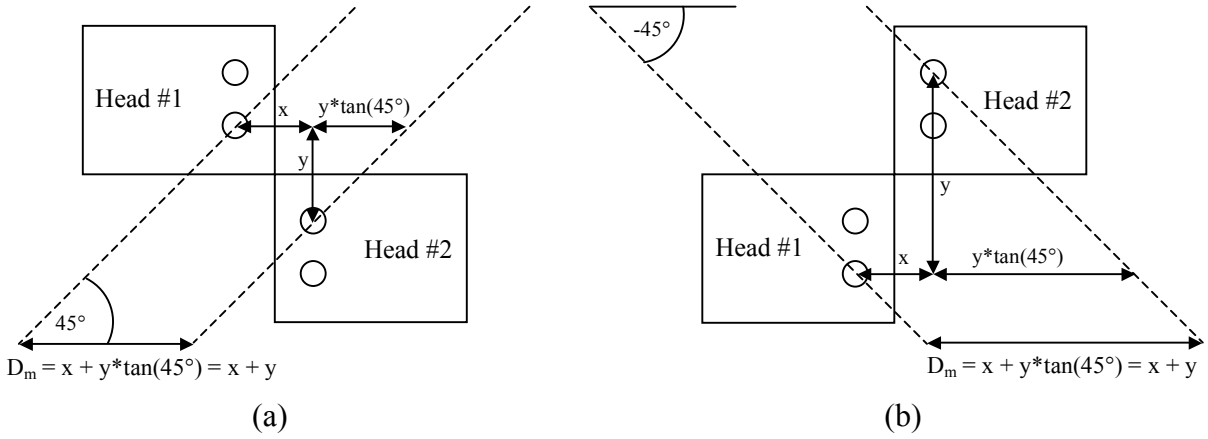

Figure 14 Two identical extrusion heads facing one another. Dashed lines indicate the toolpaths of the extrusion heads when depositing roads from a particular type of nozzle (they could be either the build or support nozzles). (a) Case where the toolpath is at +45°. (b) Case where the toolpath is at -45°.

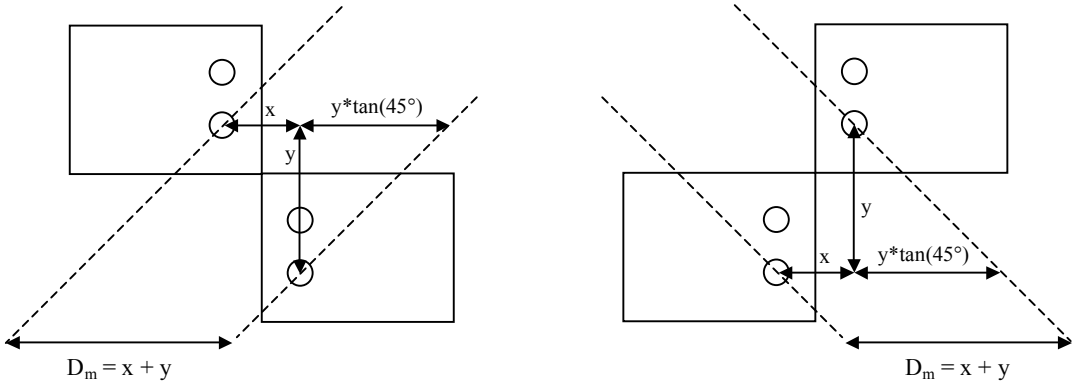

Figure 15 Case where extrusion heads that are mirror images are used. This time the minimum distance, D_m, is the same for (a) as it is for (b).

The minimum distance between extrusion heads that are next to one another can be similarly calculated using geometry. In this case the smallest distance will result from having identical extrusion heads next to each other (Figure 16), while switching the nozzles on one extrusion head will cause the minimum distance to vary depending on the trajectory angle. It is thus ideal for extrusion heads that are next to one another to be identical while extrusion heads that are across from one another should have the nozzles switched on one head so that they are mirror images of one another.

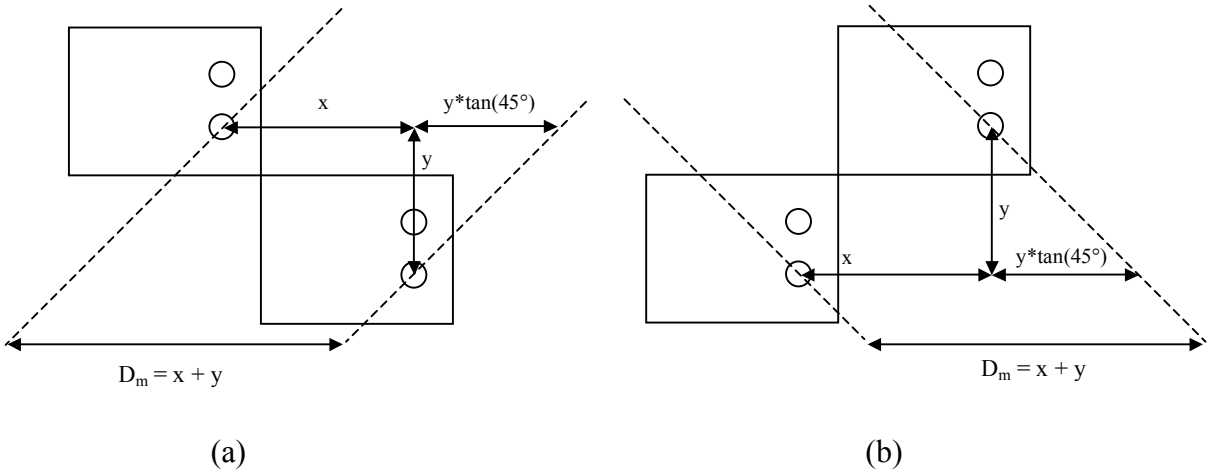

Figure 16 When identical extrusion heads are next to one another they will have the same minimum distance between them for both (a) +45° trajectories and (b) -45° trajectories.

The minimum separation between extrusion heads has been shown to depend on geometry and the design of the extrusion heads. In particular the minimum distance depends on the distance from the nozzles to the front of the extrusion head and the width of the extrusion head. In the case of extrusion heads arranged to be next to each other, the length of the extrusion head also comes into play. Careful design of the extrusion heads would thus allow the minimum separation between them to be reduced. This would likely entail orienting the extruder components, thermocouples, motors, actuators, and cooling fans so that they occupy more vertical space and less horizontal space. An extrusion head that has been optimized for a multiple head machine would thus be tall but narrow. Extrusion heads on commercially available FDM systems have approximate dimensions as listed in Table 2. The dimensions of a theoretical extrusion head that contains a vertical extruder is also listed. The commercial extrusion heads could easily be modified so that the actuator on the FDM 1600 system and the cooling fan on the Dimension SST were located elsewhere, and thus reduce their size. The minimum distance between two mirror-image extrusion heads across from each other can be found by substituting $x = 2*(b-e)$ and $y = a$ into the equation for D_m. For a FDM 1600 this

results in a minimum distance of 172 mm (6.5”); for a Dimension SST a distance of 147 mm (5.8”) is needed. By comparison, the theoretical extrusion heads requires only 82 mm (3”) of distance between their toolpaths. Substituting $x = b$ and $y = a$ into the equation for the minimum distance between extrusion heads, allows the distance for extrusion heads next to one another to be calculated. For either FDM 1600 or Dimension SST extrusion heads placed side by side, the minimum distance is 241 mm (9.4”). Again, the theoretical extrusion heads require significantly less distance between them: only 130 mm (5”). It is therefore apparent that a modification of the extrusion heads could result in a significant reduction of the distance that must be maintained between them to prevent a collision. One simple design change is to add champers to the corners of the extrusion heads. The corners typically contain only empty space so removing them would not require redesign of the internal components while at the same time allowing extrusion heads to operate closer to one another. After calculating the minimum separation between any particular set of extrusion heads, a small amount of extra space should be added to the distance between them to serve as a margin of safety to ensure that they do not rub against each other. With the physical machine’s design sufficiently specified, it is now possible to examine the calibration issues that will arise for a multiple extrusion-head FDM machine.

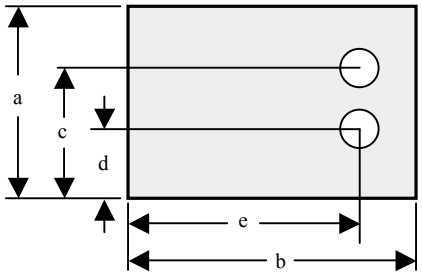

Table 2 Approximate dimensions of extrusion heads on two different FDM systems

Dimension	FDM 1600	Dimension SST	Theoretical
a	110 mm (4.3”)	113 mm (4.4”)	50 mm (2”)
b	131 mm (5.1”) (ignoring 33 mm (1.3”) actuator)	127 mm (5”) (ignoring 40 mm (1.6”) cooling fan)	80 mm (3”)
c	68 mm (2.7”)	60 mm (2.4”)	40 mm (1.3”)
d	41 mm (1.625”)	54 mm (2.125”)	16 mm (0.7”)
e	100 mm (4”)	110 mm (4.3”)	64 mm (2.5”)

3.2 Calibration Issues

There are two unique calibration issues arise for a multiple extrusion-head FDM machine that are not of concern in commercially available, single-head machines. The first issue is that the planes of motion of each X/Y stage must be coplanar, so that the roads that are laid down by different extrusion heads will lie in the same plane. If they are not coplanar, then the build will appear warped, and tight tolerances will not be achieved (Figure 17). The planes of motion should be parallel to the Z stage so that all of the nozzles have the same Z-coordinates. This will allow the use of a common Z stage.

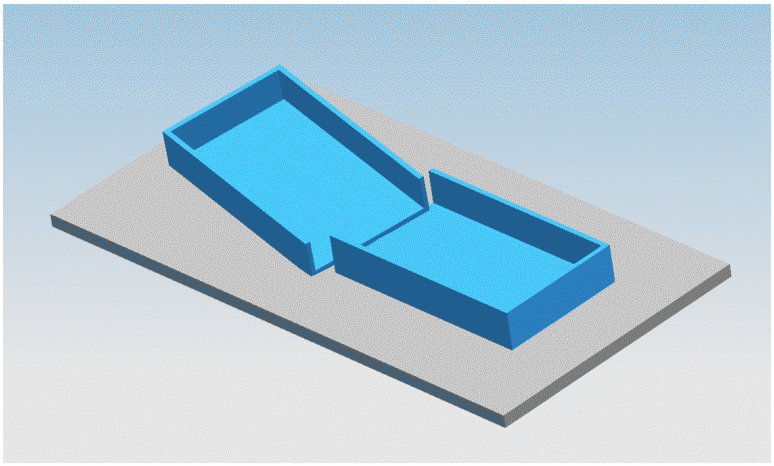

Figure 17 A warped build due to the stages not being coplanar.

The second calibration issue is caused by each X/Y stage having its own coordinate system that is used for all instructions relating to position. The coordinate system of a particular stage is referred to as its machine coordinate system (MCS). Each time that a "find home" or "find zero" command is given, such as when the FDM is turned on, the stage moves as far as possible towards the corner. That extreme point is then defined as the origin of its MCS. The X/Y stages offer high precision and repeatability in finding a specified point within their MCSs. However, before a point can be found relative to a different coordinate system (such as one that describes any point on the Z stage), the difference between the origins must be known. The differences between the origins of the MCSs used by the X/Y stages must therefore be determined and taken into account.

3.2.1 Planes of Motion and Z-Coordinate Calibration

Due to tolerance stack-up, it is not possible to simply bolt multiple X/Y stages onto a FDM frame and expect that the stages will be coplanar and with their extrusion nozzles at the same Z-coordinate. Tolerance stack-up results from the addition of the individual

tolerances of multiple components that are effectively placed in series such that a change in the dimensions of one part changes the position of the final component. There are many such components between the frame of the FDM and the tip of the nozzle. Because each component will be a slightly different size, it is possible that several larger components will be used in one X/Y stage while several smaller components will be used in a different stage within the multiple extrusion-head FDM. This results in an uncertainty about the heights of the nozzles from the Z stage and the orientations of the planes of motion of the X/Y stages.

The following calibration procedure ensures that the extrusion nozzles are all at the same Z coordinate, and that the X/Y stages are all coplanar: Each X/Y stage or group stage is suspended at the corners by bolts that pass through the frame of the FDM machine (Figure 18). A nut above the frame holds the bolts in place, and it can be used to adjust the length of the bolt and thus the height of the stage at its corner. Each extrusion head is moved in turn to each corner of its corresponding X/Y stage, and the height of the stage at that corner is adjusted until the build nozzle is a given height above the Z stage. In the case of a group stage, only one head is used. Repeating this procedure for each corner of each stage results not only in the build nozzles being a constant distance from the Z stage, but also ensures that the stages are coplanar and parallel to the Z stage.

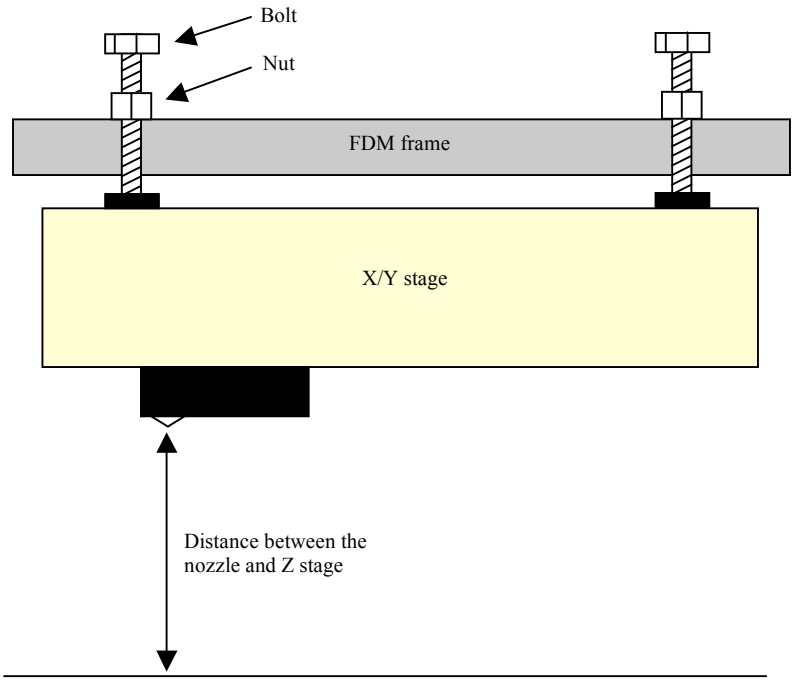

Figure 18 Illustration of a scheme for calibrating the Z coordinates of nozzles and making them coplanar.

This calibration procedure was validated by the following experiment: The X/Y stage from a FDM 1600 was mounted to a wooden frame. A felt tip marker was attached with a fixture to the extrusion head, and a poster board was located under the stage. The stage was then lowered one corner at a time until the marker made contact with the poster board. A new poster board was then placed under the stage (by lifting up on it) and the extrusion head moved to each corner of the stage, tracing out a box on the poster board with the marker. Knowing the profile of the marker, it is possible to determine how far it was pushed into the poster by measuring the width of the ink with calipers. This in turn effectively measures the height of the stage at every point that the extrusion head was moved to. The width of the ink was measured ten times on each side, with measurements being made approximately 25 mm apart. The measurements were then averaged to determine the average height of the X/Y stage on that side. A new marker was used in each experiment to avoid errors in measuring the height due to the profile of the felt tip changing as the marker was used.

Three experiments were conducted, with the variable being the angle between the frame and the table, with the front of the frame being higher than the back. In the first experiment, the wooden frame was allowed to sit flat on the table, and the stage was adjusted to be parallel to the table surface as described above. Upon measurement it was found that the front side of the stage was 0.15 mm higher than the back side. Hence, the X/Y stage made an angle of -0.029° with the table (the range of motion of the stage is 301 mm from the front to back). In the second experiment, the frame was tilted at a 1° angle, and in the third experiment it was tilted at 7° (Figure 19). After the stage was adjusted in the second experiment, it was found that the angle it made with the table was reduced to -0.068° (corresponding to a difference in height of 0.36 mm). In the third experiment, the initial 7° angle was corrected to 0.004° (corresponding to a difference in height of only 0.02 mm). Table 3 summarizes the experimental data.

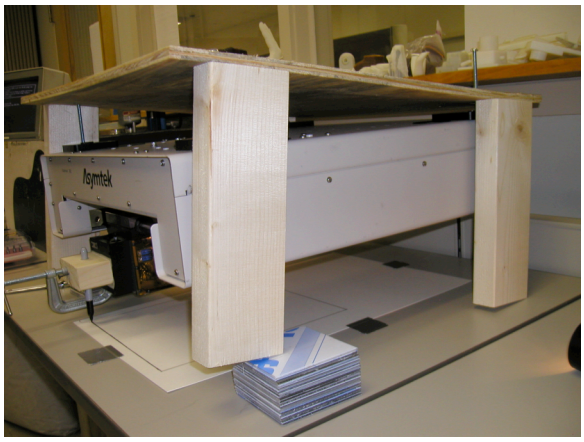

Figure 19 Experimental rig at a 7° tilt.

Table 3 The heights and angle between the stage and table before and after calibration.

Initial difference in height (mm)	Initial angle (degrees)	Difference in height after calibration (mm)	Angle after calibration (degrees)
~0	0	0.15	-0.029
5.25	1	0.36	-0.068
36.96	7	0.02	0.004

Comparing these results to a typical build layer thickness of 0.254 mm (0.01”), it can be noted that the smallest difference in height (0.02 mm in experiment 3) is only approximately 0.1 layers thick, and it is spread over the 301 mm long build volume. The largest difference in height was obtained during the second experiment, and it was approximately 1.5 layers thick (0.36 mm). This would have caused a noticeable surface discontinuity on some large parts, and it would therefore require a second calibration attempt to further reduce the angle. Ideally, the stages of a multiple extrusion-head FDM should be calibrated so that the differences in height between them is not more than 0.06 mm (1/4 the thickness of a road). This will prevent a noticeable surface discontinuity from being formed. The time required to calibrate the stage in all three experiments combined took less than an hour. Once calibrated, there should not be a need to adjust the X/Y stages further, unless the extrusion nozzles need to be changed.

The support nozzles of each extrusion head would need to be calibrated so that they all have the same Z offset with respect to their corresponding build nozzle. Otherwise the Z stage would need to move to a unique height for each support nozzle, which would prevent support material from being laid down by more than one extrusion head at a time. FDMs such as the Dimension, are capable of measuring the location of the support and build nozzles relative to each other. Systems that instead use a stop to limit the range of motion of the solenoid (that actuates the support nozzle) can be calibrated by changing the location of the stop.

There is no need to calibrate the different support nozzles to have the same X/Y offset from their respective build nozzles. This is because measuring the offset using the standard calibration technique is sufficient. In the standard technique, a small box is built and the offset measured using calipers. The user then enters the offset values into the computer, which adjusts the location of support layer coordinates by the offset amount. This is acceptable for a multiple extrusion-head FDM because each extrusion head is capable of moving independently of one another, allowing each head to have a different X/Y offset between its build and support nozzles.

3.2.2 Machine Coordinate System Calibration

The location of the origin of each stage's MCS must be known relative to one another so that the roads deposited by different extrusion heads can be properly aligned. An easy-to-implement calibration scheme is to fabricate a small box with half of the box being made by each of two adjacent extrusion heads. The deviation of the box from the desired shape can be measured via calipers to reveal the difference between the stage's origins. For example, suppose that a box is to be made with width W_0 and length L_0 as shown in Figure 20.a. The dimensions of the fabricated box (Figure 20.b) can then used to find the offset between the origins of the two MCSs used by the stages that fabricated the box. In this example the X/Y stage on the right can be observed to deposit roads lower and to the left of the roads deposited by the stage on the left. The difference between the origins in the X direction is:

$$W - W_0 = \Delta W \qquad \text{Equation 3}$$

If the roads deposited by the right stage were lower, then the difference in the Y direction will be:

$$L_0 - L = \Delta L \qquad \text{Equation 4}$$

Alternatively, if the roads deposited by the right stage were higher, the difference will be:

$$L - L_0 = \Delta L \qquad \text{Equation 5}$$

In this example, both ΔW and ΔL are negative, which is consistent with the roads deposited by the right stage being lower (the -Y direction), and to the left (the -X direction), of their intended locations. The difference between the origins is then subtracted from the coordinates for the stage on the right so that it will move to the proper location.

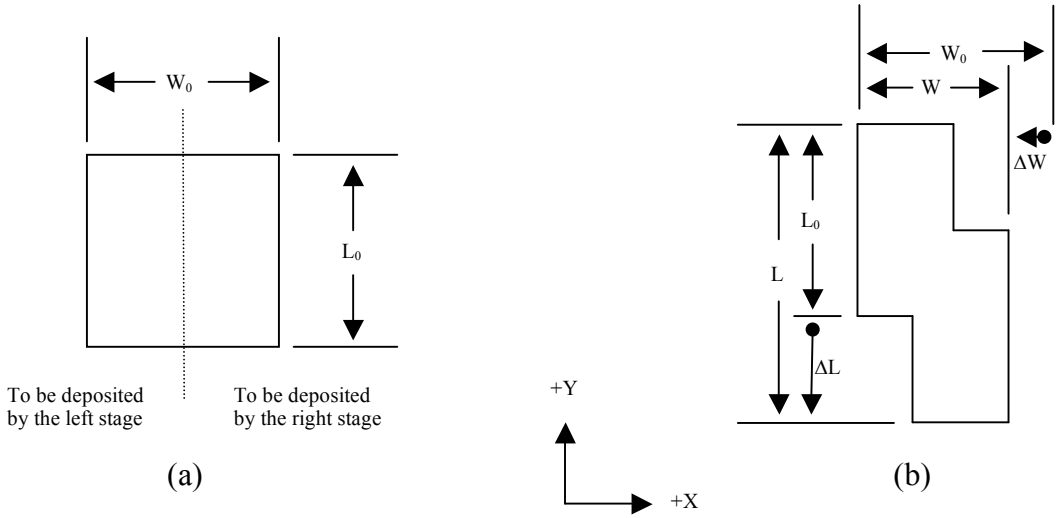

Figure 20 (a) A test box to be made by two extrusion heads with dimensions L_0 and W_0. (b) The actual test box fabricated with dimensions L and W.

In the case where there are three or more X/Y stages, then the difference in origins between each stage would be measured first as described above (Figure 21.a). The *cumulative* difference would then be subtracted from specified coordinates so that the build volumes line up properly (Figure 21.b). For example, in Figure 21, the difference between the first and second stage is (+1,+1), and the difference between the second and third stages is (+2,-1). Coordinates for the second stage are therefore corrected by:

$$-(+1,+1) = (-1,-1)$$

while coordinates in the third stage are corrected by:

$$-(+1+2, +1-1) = (-3, 0)$$

Note that in order for this calibration procedure to be used, the build volume of each stage will need to be slightly less than the plane of motion that the X/Y stage is

capable of moving within. This allows the build volumes to be aligned within the overlapping ranges of motion.

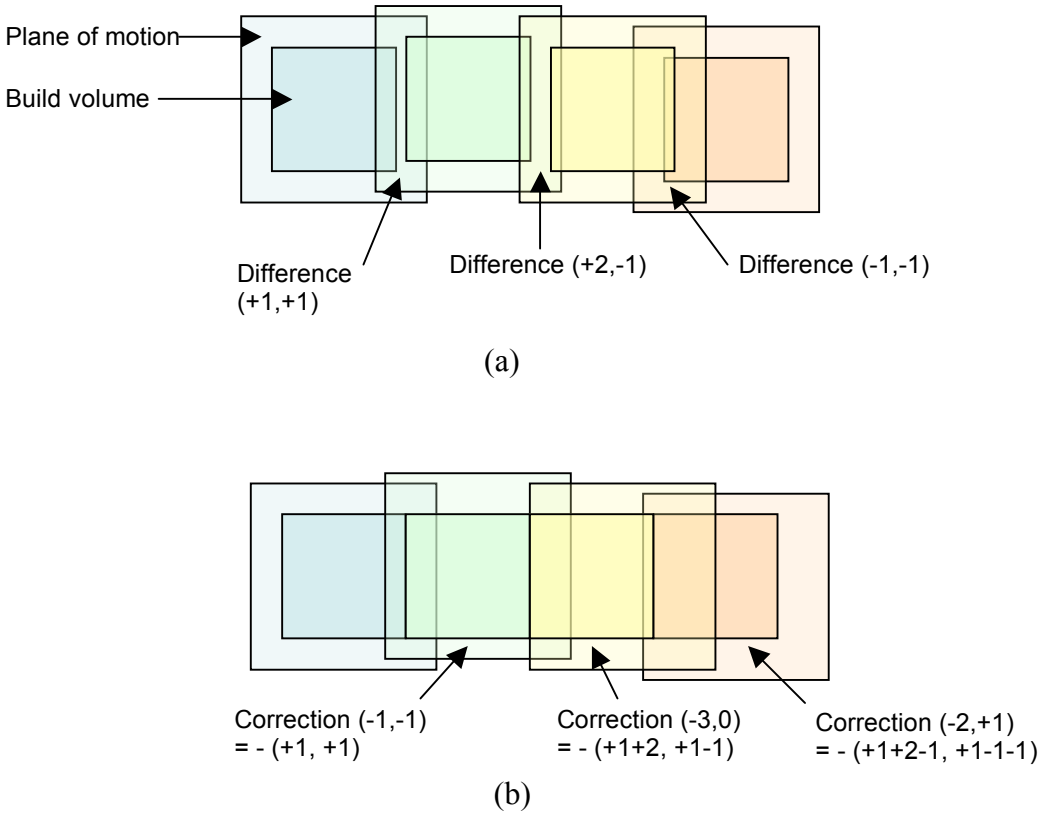

Figure 21 (a) The build volumes of four stages prior to MCS calibration. (b) The build volumes after calibration line up properly.

The X/Y stages that are used in FDM systems are precise and repeatable, and they should require only occasional calibration. In particular, following the initial assembly and installation, it should not be necessary to perform MCS calibration. Thus given the infrequent need to calibrate the planes of motion, the Z-coordinates, and the MCSs, it can be concluded that the calibration issues that arise for the multiple extrusion-head FDM as described above are not a significant detraction of such a machine.

Chapter 4

Software

The main goal of this chapter is to formulate an algorithm that will generate the toolpaths that the multiple extrusion heads will follow while depositing roads. This chapter therefore begins with an overview of the basic strategy for the toolpath generation process. It then defines new terms that will be used throughout the chapter, and then explains several important assumptions. These assumptions are used while formulating the toolpath generation algorithm, which starts with a description of how toolpaths are generated for a single extrusion-head FDM machine. The deposition of perimeter roads by a multiple extrusion-head machine is then examined, followed by the raster roads and then the shape of the seam that occurs where roads deposited at different times meet. This chapter ends with the toolpath generating algorithm, which is explained step-by-step.

4.1 Toolpath Generation Overview

While it may be expected that the toolpath generation of a multiple independent extrusion head FDM would be much more complex than that of a single head system, careful planning can simplify much of the implementation. Of primary concern is laying down roads at the highest possible speed without significantly sacrificing the mechanical strength of the part, while also avoiding any collision between the heads. Collisions between the extrusion heads must be carefully avoided because they will ruin the part being fabricated. This is because the stepper motors that drive each X/Y stage will skip steps if they face sufficient resistance to their motion. Without encoders to provide feedback to the X/Y stage controller, there is no way for the computer to know that the motor did not move as many steps as it was instructed to. This results in the collision

causing the extrusion head to be offset from the location that it is supposed to be for the rest of the build. For example, suppose that a collision results in one extrusion head moving only 7.5 mm to the left when it was instructed to move 10 mm. From that point on, the head will be located 2.5 mm farther to the right than it is supposed to be, resulting in it depositing material in the wrong locations on each subsequent layer. Thus a single collision would likely result in the entire part being ruined.

The strategy proposed in this thesis for generating collision-free toolpaths, subdivides the build volume of each layer into regions that each extrusion head can deposit without any possibility of collision. The knowledge that the heads are constantly separated by a sufficient distance to make a collision impossible, greatly simplifies toolpath generation and allows reuse of many of the same algorithms that are currently employed in standard FDM toolpath generation. This strategy is effective for multiple independent extrusion head systems, because the range of possible motions of the heads would likely only overlap in a limited region. However, while it may be tempting to simply divide the part to be fabricated into the regions accessible by the extrusion heads and then to start each head at the same side of their prospective build volume, the problem is slightly more complicated. This is because parts that are built with a clean, vertical division between the roads deposited by each extrusion head would be expected to be significantly prone to breakage at that location. Therefore some of the roads deposited by one extrusion head will need to lay overtop and bond with roads deposited by the other extrusion head on adjacent layers. The region where roads from one head overlap with those of the other head shall be referred to as the "road-overlap area" to prevent confusion with the overlap in the range of motion of adjacent X/Y stages. The location where roads laid down by different extrusion heads meet, or where roads laid down by the same head at different times meet, is referred to as a "seam."

4.1.1 Terminology

New terms will be needed to facilitate discussion of a toolpath generating algorithm for multiple independent extrusion-head FDMs. This section provides a brief explanation of most of the terms that would be unfamiliar to a reader who is generally knowledgeable about FDM. Figure 22 illustrates the new terminology.

Centerline – a line that is parallel to the long axis of the overlap in X/Y stage motion and located in the middle of the overlap.

First build-area – the first area that a particular extrusion head filled with roads on a layer. Typically, each extrusion head will have a first build-area on each layer. One of the first build-areas will be located at the seam between roads deposited by different extrusion heads, while the other first build-area will be located sufficiently far away to prevent the possibility of the extrusion heads colliding.

Midline – a line that is used to simplify calculations, the midline is located at the center of the seam width.

Overlap in X/Y stage motion – the physical space that both extrusion heads are capable of occupying.

Road-overlap area – The region where roads deposited by one extrusion head lay above or below roads deposited by a different extrusion head on an adjacent layer.

Seam – the location where roads that were deposited by different extrusion heads meet, or where roads that were deposited by the same extrusion head at different times meet. Theoretically, a seam could have any shape, although only linear seams will be considered, owing to their simplicity.

Seam width, W_s – how wide the seam is. The seam width should not be confused with the width of either of the first build-areas.

Second build-area – The second area that a particular extrusion head filled with roads on a layer. Typically, each extrusion head will have a second build-area on each layer. The second build-areas will be positioned far enough apart from one another that they can be filled simultaneously by the extrusion heads, without the possibility of a collision.

Width of the part, W_p – how wide the part is at the centerline.

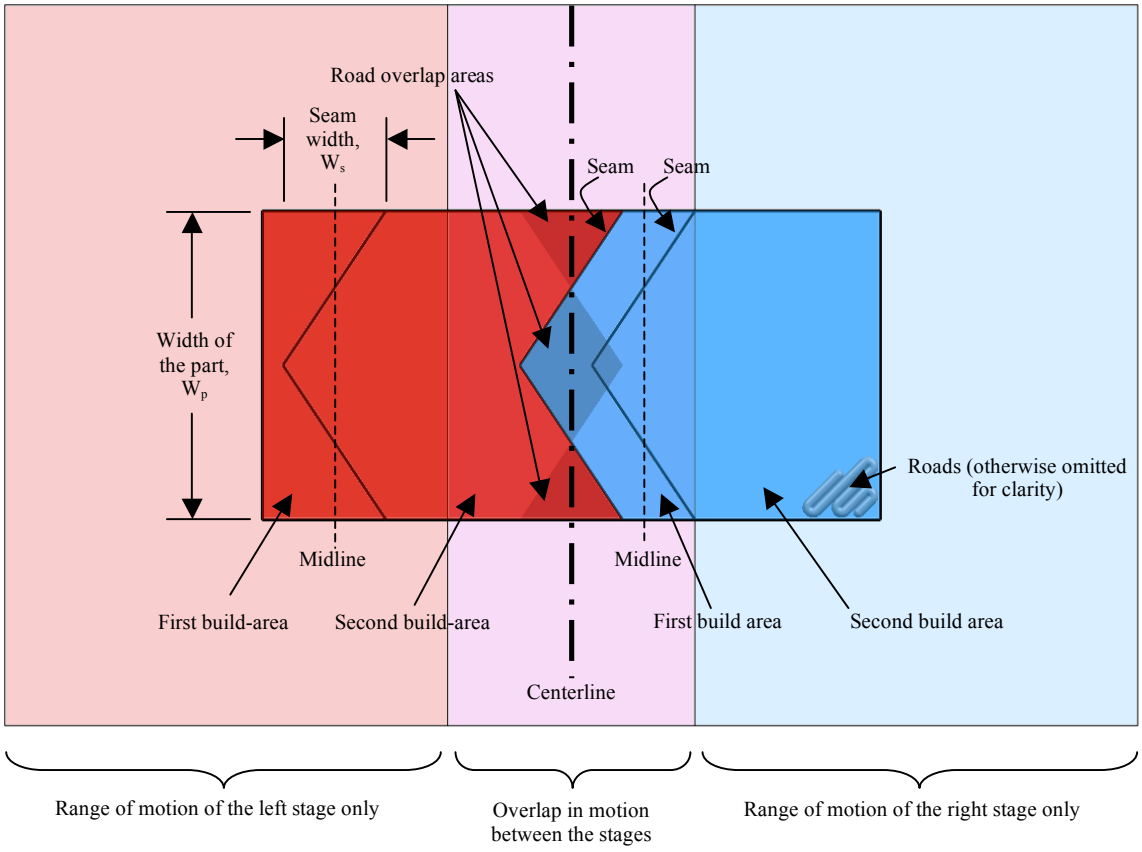

Figure 22 One layer of a rectangular part being fabricated by a FDM that has two extrusion heads. The color of the build-areas indicates which extrusion head deposited the roads within them. The adjacent layers are mirror images of this one, so that the seam between roads deposited by different extrusion heads is reversed, accounting for the road-overlap areas.

4.1.2 Assumptions

At this point, assumptions will be made that will aid in forming a toolpath generation scheme. These assumptions pertain to the way that the FDM machine will be utilized, the tradeoff between computational time and build time, and the mechanical strength of roads.

1) The computer's computational speed is sufficient that the total of all processing time is much less than the time needed to fabricate the part. Even a 10 year old computer is sufficient to generate FDM toolpaths for complex geometries within seconds. Hence, taking extra computational steps that result in a decrease in build time will generally be advantageous. Furthermore, computational steps that only *sometimes* result in a small decrease in build time will likewise be advantageous because even when these steps do not reduce build time, they will most likely only increase the computational time by an incomprehensible amount.

2) For a multiple independent extrusion head FDM, it is important to both achieve a high build rate and to fabricate mechanically strong parts. The fabrication throughput must exceed that of single head FDM systems, and without significantly reduced mechanical properties in the fabricated part.

3) It is much more likely for the fused region between two adjacent roads to fail than for either road to fail. This assumption is reached by analyzing the mechanical system formed by two adjacent and parallel roads (for more information regarding analyzing mechanical systems, see [Beer 1992] or [Beer 1996]): Consider two parallel roads viewed through their cross section and approximated as being elliptical as shown in Figure 23. Given a 0.25 mm layer thickness, the roads

would be 0.25 mm high. The thickness of the fused area depends on many factors and varies widely (Figure 24), but for the purpose of this analysis will be assumed to be approximately 50% of the road thickness. Now suppose that a load is placed on the part containing these roads and they experience a tensile force, *F*, acting perpendicular to their length. An equal and opposite force is required to prevent the roads from moving. The stress, σ, placed on the roads and fused region is:

$$\sigma = F/A, \qquad \text{Equation 6}$$

where *A* is the cross sectional area. The area of the roads will be 0.25 mm multiplied by their length, whereas the area of the fused region is approximately 0.125 mm multiplied by the same length. Given that the force is the same for the roads and fused region, the average stress in the fused region is 200% that found in the road. However, the rapidly changing surface profile at the fused region will result in stress concentration effects that may cause localized regions within the fused region to contain stress that is several times higher than the average stress. Stress concentration is a geometric effect that can be thought of as the bending of force lines as they travel from the road to the narrow fused region [Meyers 1999]. The force lines are approximately evenly dispersed in the thickest part of the road and attempt to travel horizontally until they encounter the changing surface profile, at which time they bend to remain within the material. This results in a decrease in the spacing of the force lines near the upper and lower surface of the fused region, and therefore a greater local force. The combination of the reduced cross sectional area and the stress concentration effects, is therefore expected to create areas within the fused region that experience many times more stress than found within the roads.

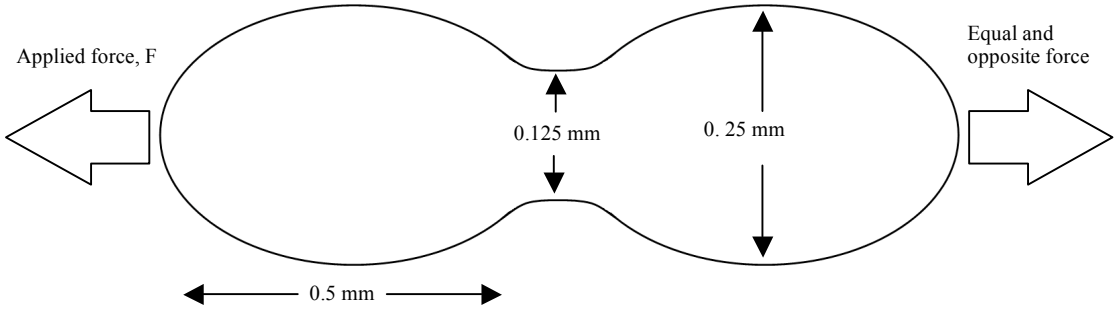

Figure 23 Two parallel roads viewed through their cross section.

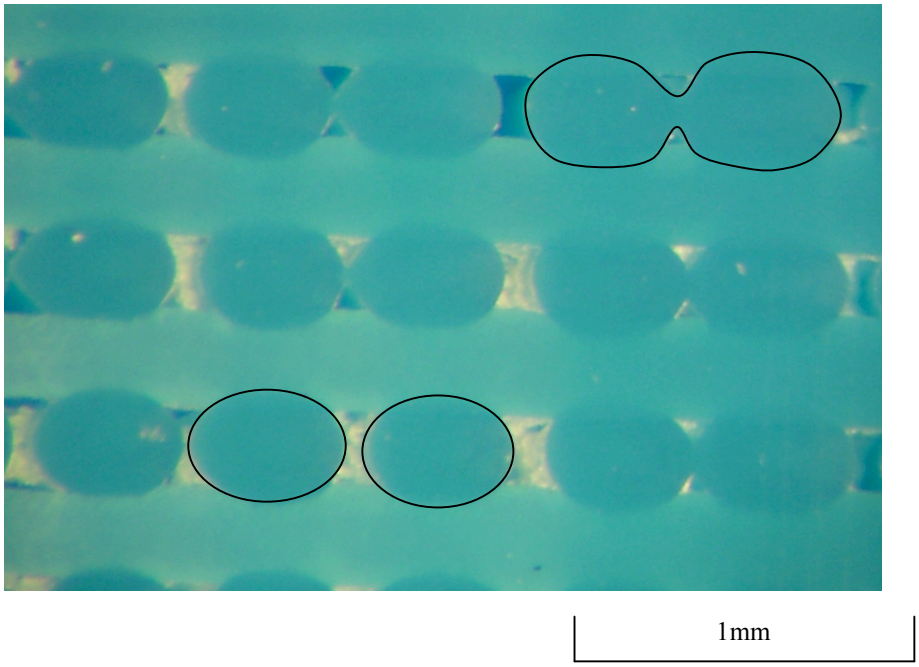

Figure 24 A microscopic image reveals a wide variety in the amount of fused area existing between two adjacent roads. Some roads share no fused area at all (outlined roads in the bottom layer), while others share a large amount (the outlined roads in the top layer share 66% of their thickness). The sample was fabricated on a FDM 1600 from ABS. The nozzle temperature was 270°C, the envelope temperature was 70°C, and the layers are 0.25mm thick. Standard Stratasys build procedures and default road spacing was used.

A material will break once its ultimate tensile stress is exceeded. Due to the much higher stress found in the fused region, it would be expected to fail

under only a fraction of the force required to break the road. Similar arguments can be presented to explain why it is desirable to reduce the amount of voids (empty space) in parts fabricated via FDM. The presence of voids both reduces the cross sectional area and leads to stress concentration, both of which reduce the strength of the fabricated part.

4) Roads are stronger along their length than width. The continuous profile of the roads down their length prevents them from being subjected to the stress concentration effects seen to act across their width in assumption #3 above. Additionally, anisotropy effects will strengthen the roads along their length while further weakening the already vulnerable fused region between them. Isotropic materials have the same material properties regardless the direction that is considered. Polymers, on the other hand, are composed of long molecules (commonly called "macromolecules" or "polymer chains") that may be aligned. A plastic that contains highly aligned macromolecules will have a higher Young's modulus (and is thus stronger) in the direction of alignment. This is because the stresses can be carried along the strong covalent bonds that are present within the large number of backbones of the polymer chains that are aligned with the stress. At the same time, the polymer will have a lower Young's modulus in the transverse direction as a result of there not being many backbones that are aligned with that direction [Rosato 1995]. Most of the stress applied to the transverse direction will initially act on the weak Van der Waals bonds between polymer chains and will pull on entangled segments of chains [Sperling 2006]. As the polymer is deformed, the Young's modulus will increase in the direction of deformation due to entangled molecules being straightened out and aligned with the direction of deformation. While this effect increases the strength some, highly oriented polymers will typically have a much higher ultimate tensile stress in the original direction of polymer chain alignment.

Roads that are deposited by a FDM are expected to contain macromolecules that are aligned along the length of the roads. This alignment is initially present in the feed stock. As the feed stock enters the extruders within the extrusion head, thermal effects will cause the molecules to relax while shear forces compete against relaxation and act to align the macromolecules. Other research groups have found that initially randomly oriented fibers placed into the filament are aligned after extrusion [Shofner 2003], suggesting that the alignment process dominates the relaxation process. As a result, roads will contain many chains that are still aligned along the road axis (Type 1 chains in Figure 25). Only a small number of chains would be expected to be found that bridge the fused region (Type 2 chains). Even a small degree of preferred orientation among the polymer chains would result in anisotropy that would weaken the fused region between roads. As the fused region is already subjected to stress concentration effects not found along the length of the roads, it will likely be the weakest point of any part fabricated by FDM.

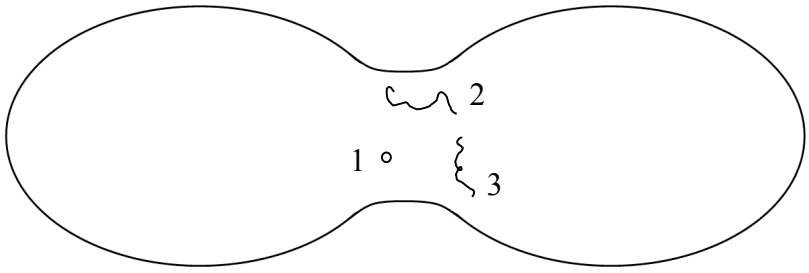

Figure 25 Illustration of the possible alignment of polymer chains within two adjacent roads.

1 = chain going into plane of the page (most common alignment)

2 = chain bridging weld

3 = chain parallel to weld

Polymer chain alignment, in combination with the weak fused region between roads, effectively explains the results that many researchers have

observed while measuring the tensile properties of samples fabricated by FDM (i.e., [Bellini 2003]). Rodríguez [2001] examined the strength of ABS parts and found the Yield strength to be 24.2 MPa along the roads but only 13.6 MPa in the transverse direction. The empirical evidence presented by various research groups thus supports assumptions three and four.

4.2 Toolpath Generation

In the case of a single extrusion-head FDM machine, the toolpath generation procedure is fairly straight forward. The model geometry is read into special software that slices it into layers. Perimeter roads are defined by linking together the line segments that define the solid/air interface on each layer. These perimeter roads may be offset inwards in order to more closely match the desired surface profile (if placed directly on the solid/air interface, they would produce a surface that deviates from the desired geometry by half a road width). Infinitely long rays with zero radius, called "dexels," are then intersected with the geometry on each layer [Zhu 2002]. The dexels are spaced apart with a distance equal to the road width and are oriented by 90° from one layer to the next. The dexels are then truncated to lie only within the solid material, and are then reduced in size further by the width of a road so as to allow space for the perimeter roads. Small line segments are added to connect the dexels, forming a continuous set of lines that are used for the toolpath of the raster fill.

For simple geometries a single, continuous toolpath that fills the entire internal area is often possible. However, in the case of more complicated shapes (particularly hollow parts) there will be an area that cannot be reached without stopping the road, moving the extrusion head to a new position, and then beginning a new road. The term "complex toolpath" is used here to describe the resulting toolpath for the case where more than one road is needed to fill the internal area, whereas a "simple toolpath" fills the entire internal region with one continuous road. In most cases, a complex toolpath is not

much more computationally difficult to calculate than a simple one. The main difference is that in the complex case the toolpath has multiple start/stop locations, and it involves moving the extrusion head to a new location to start each new road. In both the simple toolpath and complex toolpath cases the same rules for determining the start/stop locations can be used. For example, consider the algorithm where the start point is located at the lowest, rightmost dexel endpoint. The toolpath would then follow along up the dexel, across the short line segment that attaches it to the adjacent dexel (on the left), down that one and so on until it reaches a dexel endpoint without any more dexels to the left that can be connected by a line segment without crossing the boundary of the region to be filled (Figure 26.a). If the toolpath was simple, then the entire interior region would be accounted for and no unused dexels would remain. If the toolpath was complex, then the dexel segments that have already been used would be ignored and the process repeated from the next lower, rightmost dexel endpoint until the entire interior region has been accounted for (Figure 26.b).

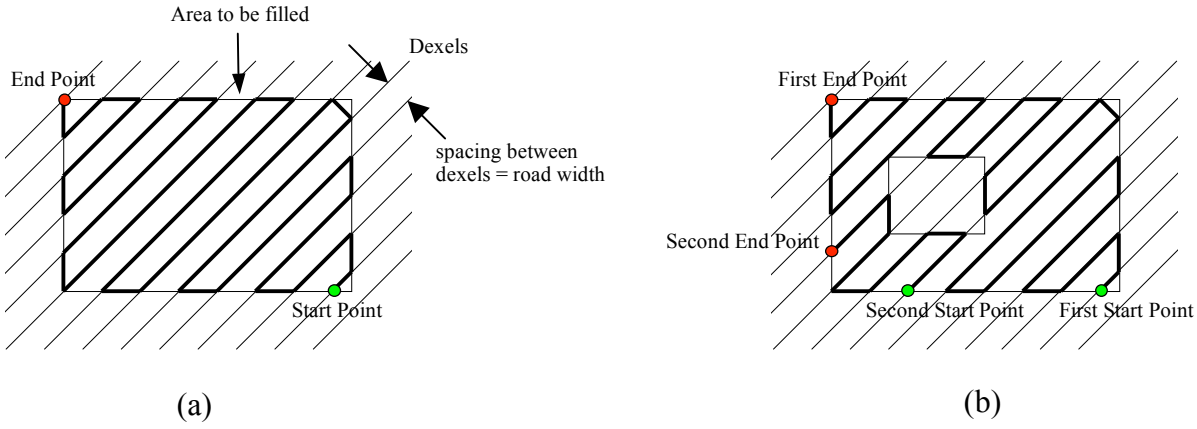

Figure 26 (a) Simple toolpath for a rectangular solid. (b) Complex toolpath for a solid containing a rectangular hole.

The overall toolpath generating procedure for a multiple extrusion-head FDM machine is similar to that of a single-head machine. Differences first occur after the

CAD model is sliced into layers. When a multiple extrusion-head FDM machine deposits perimeter and raster roads, it will need to do so differently than a single extrusion-head machine due to different areas being deposited by different extrusion heads. Seams will occur where roads deposited by different extrusion heads or at different times meet. The toolpath generating algorithm will also need to optimize the fabrication process so that the lowest fabrication time is obtained.

4.2.1 Perimeter Roads

The following will consider which, of two approaches for depositing perimeter roads by a multiple independent extrusion head FDM, will produce the highest surface quality. The first approach is to surround the entire build area of each head with a perimeter, resulting in perimeter roads contained within the bulk of the solid part. The second approach is to define a start point for each extrusion head that coincides with the end point of a different head so that a single perimeter is generated as in the case of a single extrusion head FDM, only with additional start/stop points.

When internal perimeters are used, a significant deviation from the intended surface can be observed to occur where the internal perimeters meet (Figure 27). The deviation is caused by fillets that are added to sharp corners by the FDM. These filets are due to both the inability to exactly control the location of the extrusion head when rapidly changing directions (due to momentum) and the round orifice of the nozzle. The radii of the filets are on the same order of magnitude as the road width, and two fillets occur next to each other, one from each extrusion head.

Multiple end points will also cause surface discontinuities due to the shape of the road when it is started or terminated (Figure 27). Calibration of the road's endpoints is already required, and if performed properly, can reduce surface discontinuities to a minimum. This results in a much smaller deviation from the intended surface than in the

case of when an internal perimeter is used. Therefore interior perimeter roads should be avoided and perimeter roads made with multiple start/stop points should be used instead.

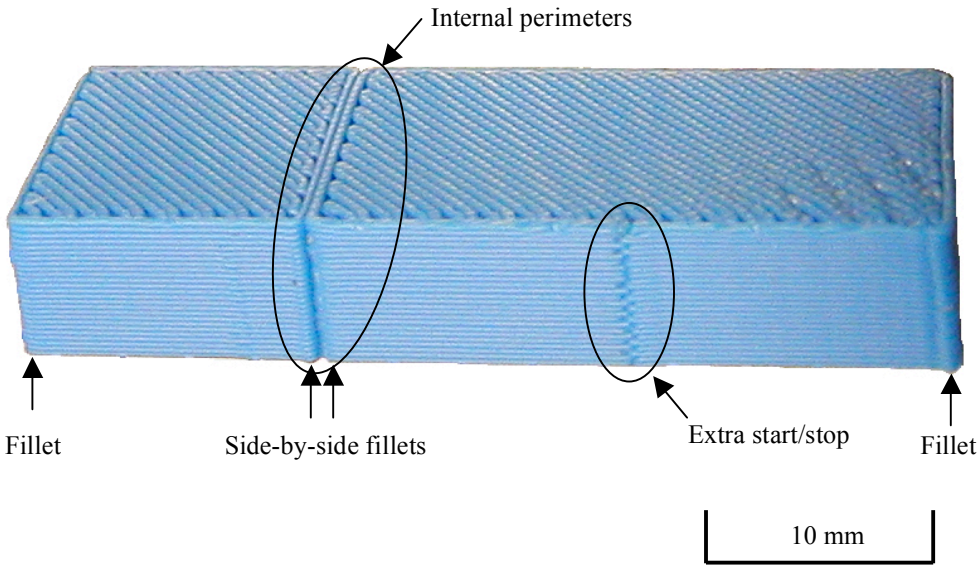

Figure 27 Photograph of a sample made with internal perimeters and an extra start/stop point in the perimeter. Note the fillets added by the FDM at the corners, which are sharp in the CAD model. The two adjacent fillets at the internal perimeters are visible by the naked eye at a distance of approximately 2 meters while the extra start/stop is only noticeable under close inspection.

4.2.2 Raster Roads

With the previously listed assumptions (section 4.1.2) it becomes possible to consider the raster pattern best suited for a multiple independent extrusion head FDM. The ideal pattern should rapidly produce parts that have a high strength given assumption #2 that both strength and speed are important. The fastest build time will result from cooperation between the extrusion heads to simultaneously deposit different areas of the raster pattern without one head having to wait for the other one to get out of the way. In order to achieve simultaneous deposition, it is important that each head builds as close to the same amount as possible. It will also be required for the build area of each layer to be divided

into smaller areas within which the extrusion heads can deposit material without any possibility of a collision. As this will result in multiple seams, it is important that the raster pattern effectively transmits stress across the seams. Assumptions 3 and 4, when considered together, lead to the conclusion that the case where many fused regions align vertically should be avoided. This is because the alignment of fused regions on subsequent layers would create a weak point in the part. The raster pattern should also produce a part with few voids and roads that are positioned so as to transmit as much force as possible along the length of the roads as opposed to through their thickness. Traditionally the raster pattern alternates by 90° each layer so that roads on one layer do not lie directly along the roads below them, but instead are perpendicular. This allows the strength of the roads on one layer to compensate for the weak fused regions in the layer below it.

There are two configurations of interest that allow the long axis of roads to lie at 90° from one layer to the next. The first configuration is when the roads lie at 0°/90° relative to the "centerline." The centerline is a line that is parallel to the long axis of the overlap in X/Y stage motion and located in the middle of the overlap (Figure 22). The second configuration is when the roads lie at +/-45° relative to the centerline. Figure 28 illustrates the difference between a 0°/90° raster pattern and a +/-45° raster pattern. While these two configurations are normally equivalent via a 45° revolution about the Z-axis of the part inside the build volume, they are not equivalent in this case due to the road overlap. Comparing an arbitrary geometry containing a 0°/90° raster to one containing a +/-45° raster (Figure 29.a and b), a major drawback to using 0°/90° roads can be observed. As can be seen in Figure 29.a, there is an area where the fused regions of all the layers in the 0°/90° part stack up on one another. At the same time, the 0° oriented roads deposited by the first head (represented by darker/red roads) only overlap with the 90° roads that the same head deposited on the adjacent layers and do not strongly interact with any roads deposited by the other head. The 0° roads deposited by the second head (represented by lighter/blue roads) only interact with 90° roads on adjacent layers and therefore can only transmit axial stress to the 0° roads deposited by the first head through the weak fused regions of the 90° roads above and below it. This is

expected to make the seam very weak regardless of the magnitude of road overlap, as axial stresses acting on the 0° roads are concentrated onto the fused regions of every other 90° layer.

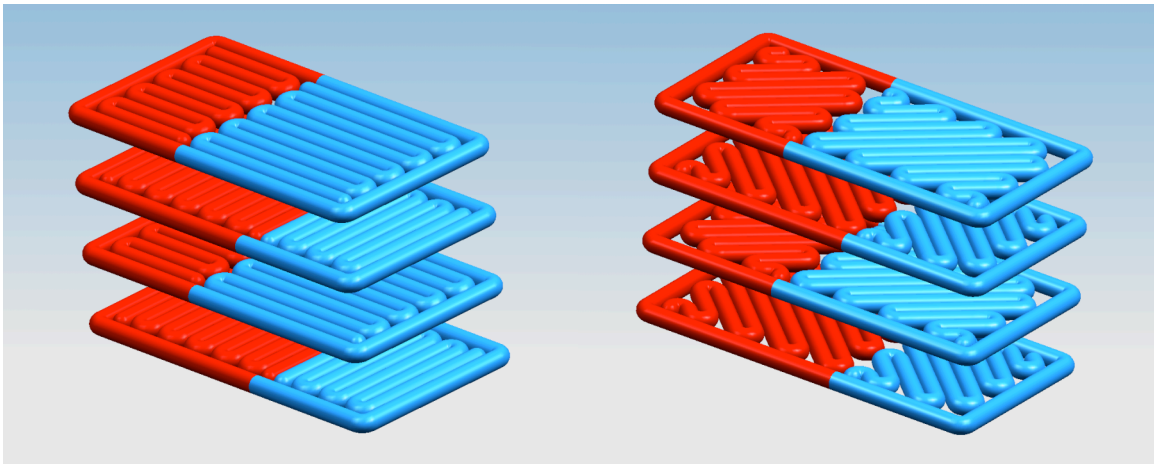

(a) (b)

Figure 28 (a) A 0°/90° raster. (b) A +/-45° raster. The color of the roads indicates which head deposited them.

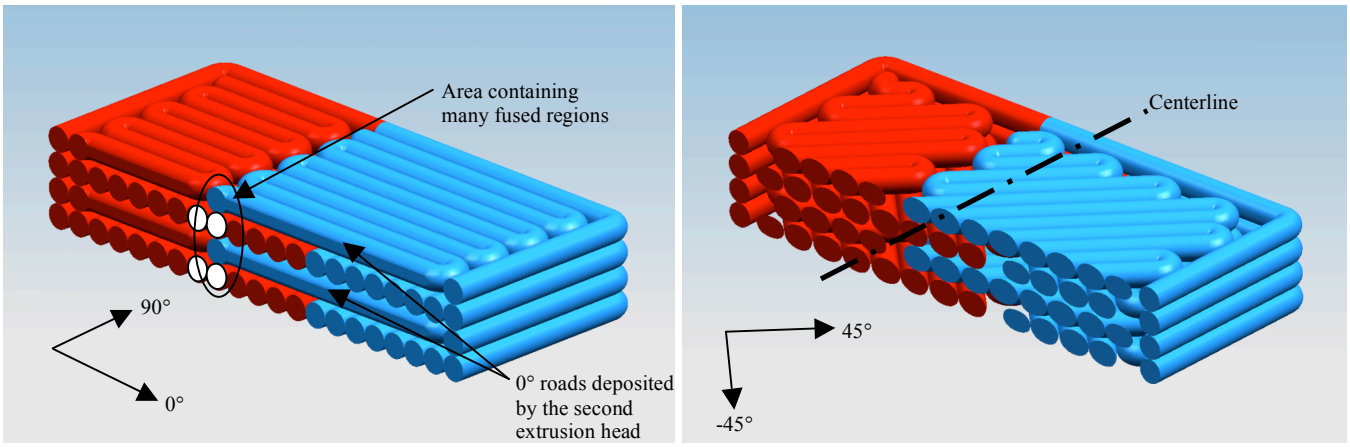

(a) (b)

Figure 29 (a) Cross section view of a part fabricated with a 0°/90° raster. The color of the roads indicates which head deposited them. Note the area containing many aligned fused regions where the roads change directions. 0° roads deposited by the second head transmit their stress through the fused region between the 90° roads deposited by the first head (white cross-section areas). (b) Cross section view of a part with a +/-45° raster.

The +/-45° raster (Figure 29.b), on the other hand, does not display any of these negative behaviors. Its +45° roads overlap with -45° roads deposited by both heads on the adjacent layers. Stress that is transmitted axially along the roads is transmitted across the seam through the intimate contact that exists between roads deposited by different heads. This allows the stress that is transmitted through the seam to act on the fused regions between several roads instead of being concentrated on a single fused region as in the previous case. Therefore the preferred raster pattern should be composed of roads with a +/-45° orientation relative to the centerline.

4.2.3 Seams

Because the road overlap is required to increase the mechanical properties of the part, the shape of the seam should be chosen so as to encourage roads deposited by one head to strongly interact with roads deposited by the other head. A seam orientation that is 90°

relative to the centerline produces little contact between roads deposited by different extrusion heads on the same layer. The opposite extreme is a seam that is at 0°. A 0° seam is useless because most parts of interest will likely be considerably larger than the width of overlap in X/Y stage motions. The result being that the heads will be incapable of reaching all the locations where roads need to be deposited. Seams created at almost any angle between these two extremes (0° and 90°) will cause many locations where the raster pattern roads will need to change directions, resulting in locations where there is little contact between roads deposited by different heads on the same layer. The exception is the case where the seams alternate each layer between +45° and -45°. In this case, the seams line up with the raster pattern! The result is that the roads appear nearly the same as they would if the part was fabricated by just one extrusion head (Figure 30).

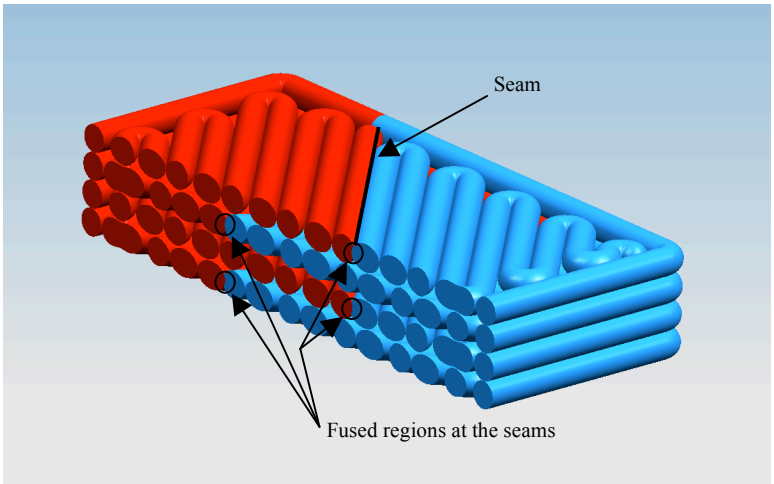

Figure 30 Cross sectional view of a part made with a +/-45° raster with seams also alternating between +/-45°. The color of the roads indicates which head deposited them. Note that a fused region between roads deposited by different extrusion heads occurs at the seams.

A 45° seam orientation has many advantages, such as the elimination of voids at the seams. The nearly identical road layout compared to those deposited by a single extrusion head is expected to yield very high strength parts. Also, the 45° angle makes it

easy for each head to deposit the same amount of roads. By simply positioning the seam in the middle of the geometry to be deposited on the layer, each head will be responsible for depositing roads in equal build areas as a consequence of geometry. This is a big advantage, as it allows both extrusion heads to deposit material simultaneously, reducing the build time to the smallest possible amount. Of course an approach will be required to prevent collisions between the heads, but that will be considered below. The seam can be observed to contain a fused region between roads deposited by different heads (Figure 30). This further increases the strength of the part because roads interact with those deposited by the other head on the same layer in addition to interacting with roads on adjacent layers.

The problem with utilizing a seam that is at 45° is that the seam's width will be greater than the overlap in stage motion if the part to be fabricated is sufficiently large. This will lead to the extrusion heads not being able to deposit material everywhere that they are supposed to. In order to prevent this, it is necessary to keep the seam within the region of overlap between the two X/Y stages (Figure 22). A simple approach to accomplish this is to change the direction of the seam once it reaches the desired width (Figure 31.a). By alternating the angle of the seam between +45° and -45°, it will continue to line up with the roads once it changes directions a second time.

Road overlap will occur even if the location of the +/-45° seam is shifted in a direction that is perpendicular to the centerline (Figure 31.b). This is a useful fact to exploit, as it allows the location of the seams to be offset from one layer to another. Changing the location of the seams allows the build area of each extrusion head to be kept equal if the center of the part geometry moves from one layer to the next (as in the case of a simple ramp). The location of the seams cannot be allowed to be shifted parallel to the centerline or else the amount of road overlap will be reduced. As can be seen in Figure 31.c, if the seam is shifted by an amount equal to the width of the road overlap, then none of the roads deposited by one head will lie on roads deposited by the other head. This results in the elimination of the road overlap, and is expected to greatly

reduce the strength of the part. As there is no reason why the seams should ever be shifted this way, it is cause for no concern.

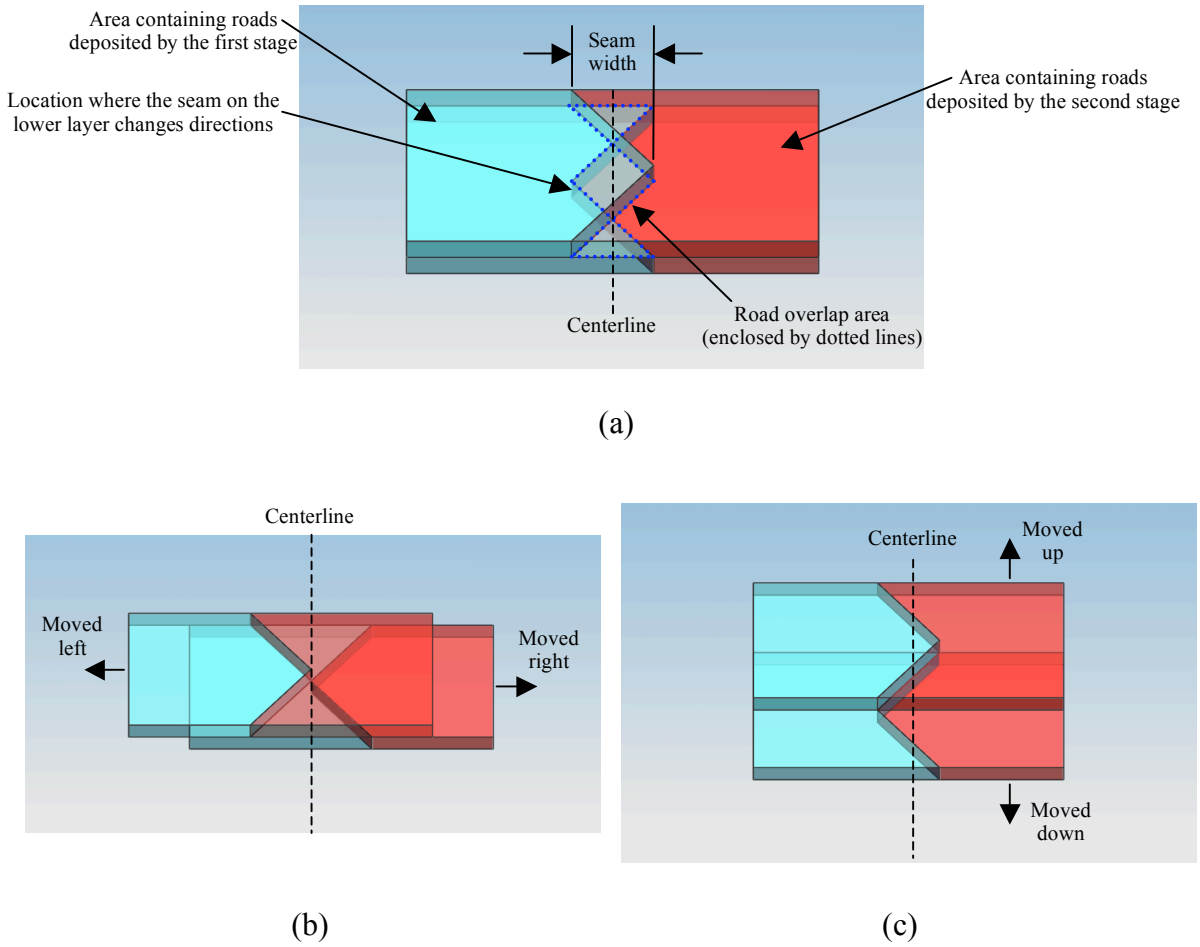

Figure 31 (a) Two layers with seams that are located at the same location. (b) The case when the top layer is shifted to the left by an amount equal to the half the seam width. The displacement is in a direction perpendicular to the centerline. Note that the road-overlap area increases. (c) The case where the top layer is shifted parallel to the centerline by an amount equal to half the seam width. In this case the roads deposited by one head do not overlap with those deposited by the other head, and there is thus no road-overlap area.

The insertion of seams into a part will likely have an effect on the fabricated part's mechanical strength. Based upon the assumptions made in Section 4.1.2, it can be theorized (1) that the strength of the part will be greatly degraded if little or no road

overlap occurs at the seam, and (2) that the larger the road overlap, the stronger the seam will become. Fabricating acceptably strong parts therefore requires the prerequisite of understanding the relationship between the magnitude of the road-overlap area and the seam width. Geometry can be used to find the *minimum* road-overlap area, A_{min} for a given seam width:

$$A_{min} = W_s * \tfrac{1}{2}W_p \qquad \text{Equation 7}$$

Where W_s is the seam width and W_p is the width of the part measured parallel to the centerline. This minimum overlap area occurs when seams from two adjacent layers are located at the same position. In the common case when seams on adjacent layers do not lie directly over one another, the road overlap will be increased.

The relationship between road-overlap area and the strength of the part is best described from empirical data. This is because the interplay between the shape of the roads, their orientation, and their anisotropic properties makes formulating a meaningful model based on mechanical theory alone difficult. In order to examine the relationship, six tensile bars were fabricated for each of six different cases, each case having a different amount of road overlap area. Tensile bars conformed to ASTM standards [ASTM] and were fabricated with a FDM 1600 with a T12 tip. The tensile bars were 13 mm (0.5 inches) wide, 6.35 mm (0.25 inches) thick, and had a gage length of 50 mm (2 inches). The default layer height of 0.254 mm (0.01 inches) was used in combination with the default road width of 0.508 mm (0.02 inches) and default road spacing. The standard Stratasys build procedure (revision 2.0) was used. Tensile testing was performed using a MTS 500 kN machine with a cross head speed of 1.27 mm/minute. An extensometer was used to measure strain. All samples were fabricated from commercially available acrylonitrile butadiene styrene (ABS) filament available from Stratasys Inc. under the product designation “P-400”. Prior to use, the filament was dried under vacuum at 75°C for 4 hours. The extrusion head temperatures were 270°C for the main material and 265°C for the support material, while the build envelope temperature was 60°C.

In order to simulate a multiple extrusion-head machine, the numerical control code was modified so that the extrusion head would first deposit the perimeter roads belonging to one head and then deposit the perimeter roads belonging to the other head (no internal perimeter walls were made). Perimeter roads started and stopped at the seams. The FDM would then deposit the raster roads belong to each head separately, alternating from one layer to the next between 45° and -45°. Likewise, the seams also alternated between +45° and -45°. The tensile specimens that were fabricated were therefore identical to those that would be produced by a two-head machine. This in turn allows for the effect of inserting a seam into a part to be investigated. Six samples were fabricated for each of the six cases, each case having a different amount of road overlap area. In the first case, the tensile specimens had a seam width of zero, resulting in there being no road overlap (Figure 32). In the second case (Figure 33), the seam width was 3.175 mm (0.125 inches), resulting in a road overlap of 20.2 mm^2. The third case (Figure 34), had a seam width of 6.35 mm (0.25 inches) and road overlap area of 40.3 mm^2. The seam was 12.7 mm (0.5 inches) wide in the fourth case (Figure 35), resulting in 80.6 mm^2 of road overlap area. The fifth case also had a seam width of 12.7 mm, but the seams were offset 28.6 mm from one layer to the next in order to create 443.6 mm^2 of road overlap area (Figure 36). The sixth case was fabricated with a single perimeter road and did not contain any seams (Figure 37). This allows the sixth case to serve as the control for comparison to the strength of a part fabricated with only one extrusion head. It also represents the case when the road overlap area is equal to the narrow section's length multiplied by the width, which is 806.5 mm^2. In the illustrations of the different cases, the blue areas represent perimeter and raster roads deposited separately from the roads within the red areas such that the tensile specimens are fabricated the same way that they would be if two extrusion heads were used. Also, the lines indicate the primary direction of the roads, but the short segments connecting them are not shown, nor are they to scale (the actual spacing is about the same as the thickness of the lines).

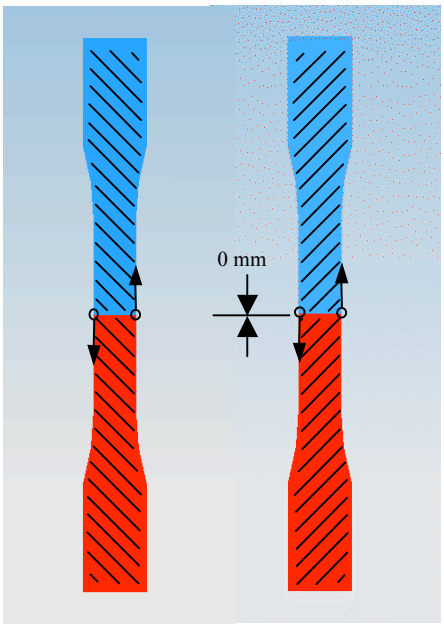

Figure 32 In the first case, the seam width was zero, resulting in no road overlap. The perimeter roads started and stopped at the seams (arrows).

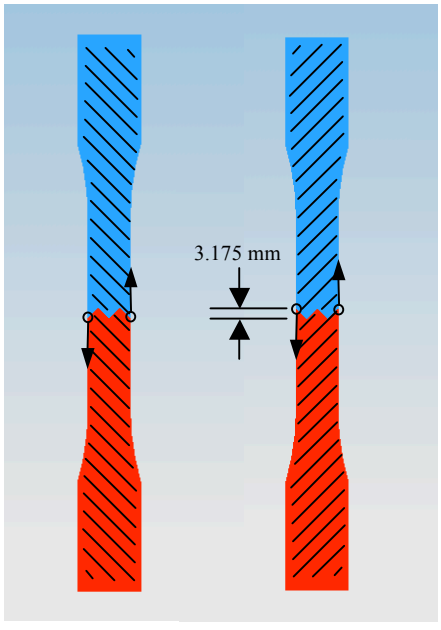

Figure 33 In the second case, the seam width was 3.175 mm (0.125 inches), which is a quarter of the width of the tensile bar. This resulted in 20.2 mm^2 of road overlap area. The perimeter roads started and stopped at the seams (arrows).

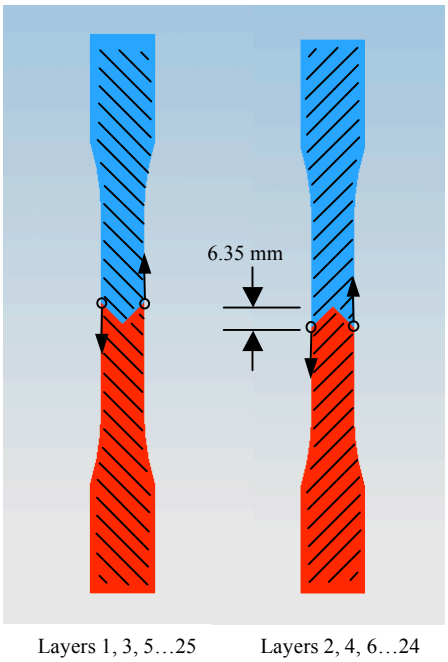

Figure 34 In the third case, the seam width was 6.35 mm (0.25 inches), which is half of the width of the tensile bar. The third case had 40.3 mm^2 of road overlap area. Perimeter roads started and stopped at the seams (arrows).

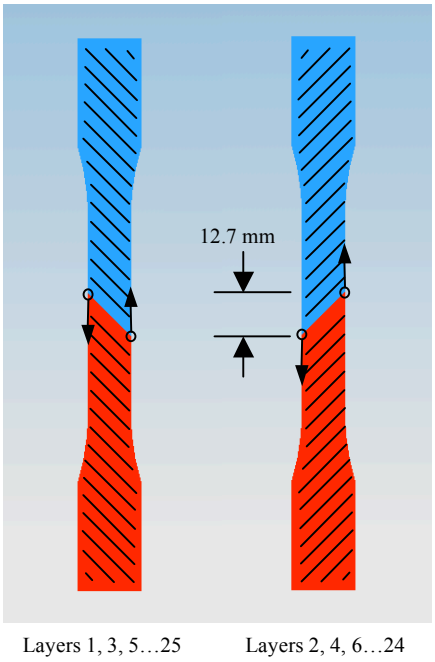

Figure 35 In the fourth case, the seam width was 12.7 mm (0.5 inches), resulting in 80.6 mm^2 of road overlap area. The perimeter roads started and stopped at the seams (arrows).

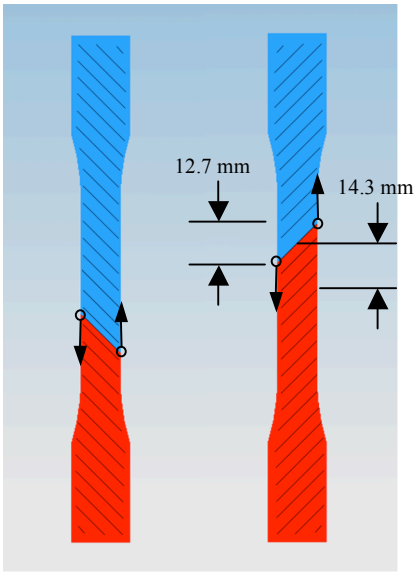

Figure 36 In the fifth case, the seam width was 12.7 mm (0.5 inches) but was moved 14.3 mm from the center of the bar to create 443.6 mm^2 of road overlap area. The start/stop point of the perimeter roads are indicated by arrows.

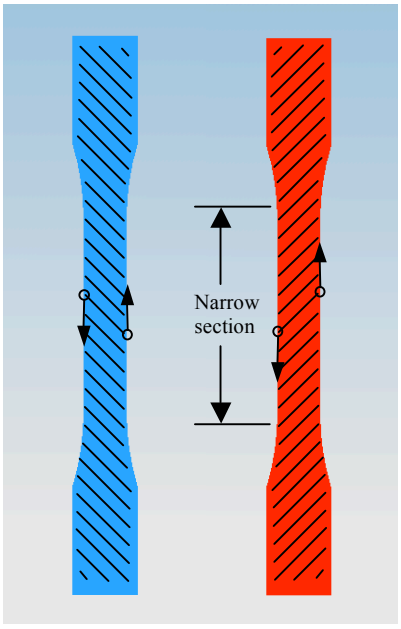

Figure 37 The sixth case was the control and had no seam. It has 806.5 mm^2 of road overlap area, which is equal to the narrow section's length multiplied by the width. The start/stop point of the perimeter roads is indicated by arrows.

Visually comparing the six tensile cases allowed some observations to be made. The fourth, fifth, and sixth cases could not be visibly discerned and the extra start/stop of the perimeter roads in most samples could not be seen from a distance beyond 1m. The extra start/stop points were manifested as small discontinuities in the surface profile (the surface would smoothly curve slightly inwards there). The conclusion that including extra start/stop points in the perimeter roads do not significantly detract from the surface finish of the fabricated part is therefore justified.

Samples from the first case were extremely easy to break. Four of the six such tensile bars broke as they were removed from the support material. One sample broke as it was casually handled, and the sixth tensile bar broke as it was being loaded into the tensile testing machine. It is therefore obvious that the inclusion of at least some road-overlap area is an important requirement of any part to be fabricated by multiple extrusion heads.

The road-overlap area has been calculated for cases 1-4 using Equation 7. In the sixth case, the effective road overlap area is equal to the narrow section's length multiplied by the width. Pertinent data from the tensile tests is compiled in Table 4 and then plotted in Figure 38. In lieu of tensile data for the first case, where there is no road overlap, the strength and ductility has been estimated to be approximately zero. This is based on the ease at which these tensile bars unintentionally broke and the fact that they broke in such a brittle manner.

Table 4 Summary of tensile data.

Case #	Road-overlap Area (mm^2)	Average Maximum Stress (Mpa)	Standard Deviation (Stress)	Average Maximum Strain (mm/mm)	Standard Deviation (Strain)
1	0	~0	n/a	~0	n/a
2	20.2	5.92	1.30	0.011	0.0023
3	40.3	9.76	0.95	0.015	0.0028
4	80.6	11.74	0.36	0.023	0.0012
5	443.6	11.69	0.40	0.052	0.0035
6	806.5	11.99	0.43	0.068	0.0036

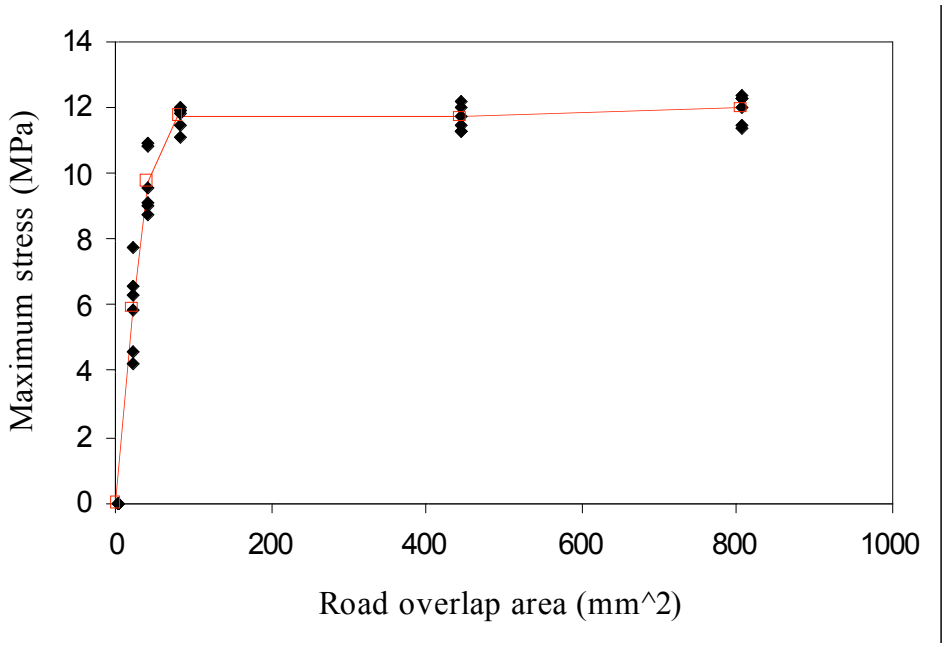

(a)

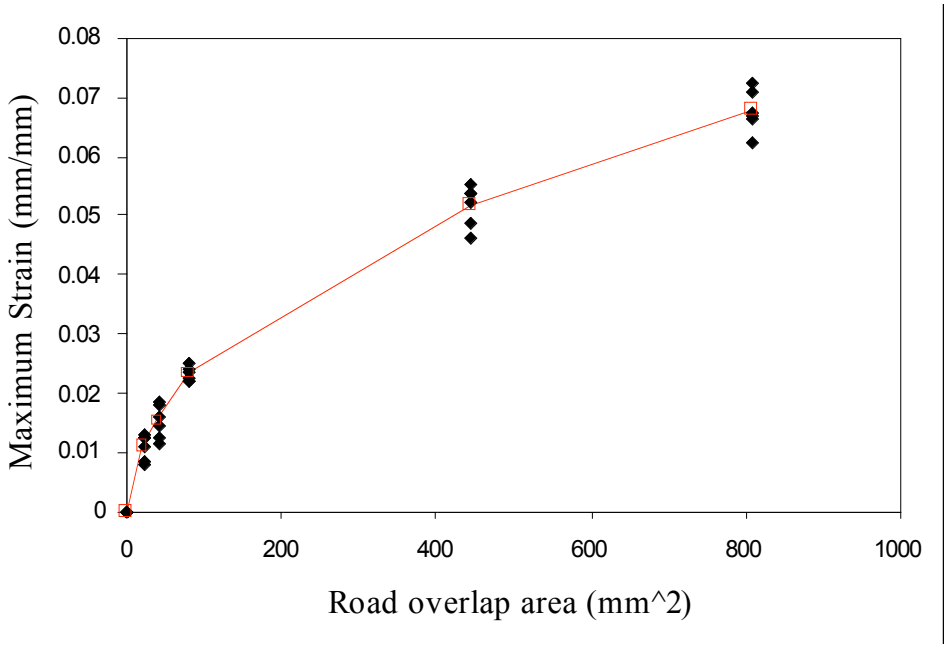

(b)

Figure 38 (a) Maximum tensile stress versus road-overlap area. (b) Maximum strain versus road-overlap area. Lines connect the average values, which are indicated by hollow squares.

From the plot of the stress versus road overlap (Figure 38.a), it appears that the strength of a part containing a seam asymptotically approaches the strength of a part without any seam after the road-overlap area is increased beyond a critical threshold. This threshold is likely related to the efficacy of the roads to transmit forces to perpendicular roads on adjacent layers through the limited contact area between them. The strength of the part can thus be conceptualized to increase with increasing road-overlap area due to roads deposited by one head being bonded to more roads on adjacent layers from the other head. As a road bonds with roads from the other extrusion head, each new bond is perhaps capable of bearing a small fraction of the axial forces needed to break the road. The limiting factor that determines the strength of the part would therefore be the strength of the contact points between the roads multiplied by the number of contact points. Increasing the overlap area increases the number of contact points, and therefore would increase the strength of the part. Once enough contact points have been formed that the combined strength of the contact points exceeds the strength of the road, increasing the number of contact points further would not add to the strength as the road will break before the contact point do. Ergo the fourth case has nearly the same strength as the fifth case.

Each of the samples from cases 2-6 had a Young's Modulus of approximately 1,200 MPa. Each sample also could be observed to yield under just less than its maximum stress. During yielding, molecules move past one another, typically resulting in the tensile bar being deformed under approximately constant stress. A comparison of the maximum strains that the samples endured prior to failure (Figure 38.b), reveals that the maximum strain increases as the amount of road overlap increases. This trend is most likely due to stress concentration effects that occur at the contact points between roads deposited by different extrusion heads. As the tensile bar deforms, the contact points experience shear forces that would cause them to also distort. These shear forces are caused by roads deposited by one extrusion head being pulled in the opposite direction as the roads that were deposited by the other extrusion head. The contact points that link the roads together thus experience force vectors that are oriented in opposite directions but separated by a small distance, just like the forces experienced by paper as it is cut with a

pair of scissors. The resulting deformation would reduce the cross sectional area of the contact points, which in turn increases the stress contained within them, and thus resulting in more deformation. The increased number of contact points present in a larger road-overlap area will distribute the stress over a larger area and will thus be less susceptible to the stress concentration effect.

With the tensile data analyzed, it is now possible to evaluate the seam width that should be used to ensure that the minimum road-overlap area is sufficiently large to provide adequate strength. Recall that Equation 7 relates the seam width to the minimum road-overlap area. From the tensile data (Table 4), it can be observed that the strength of the part dramatically increases as the road-overlap area is increased up to the critical threshold. Beyond the critical threshold, the strength of the part is nearly constant. For this reason the seam should be at least wide enough to produce a minimum road-overlap area that equates to the critical value of 80.6 mm^2 for a 12.7 mm wide part. A seam width that is equal to or greater than 12.7 mm (0.5 inches) will therefore suffice. Such a seam will allow the fabricated part to be strong enough that the difference in strength will not be apparent to users when comparing parts made on a multiple extrusion head FDM to a parts made on a single extrusion head machine.

The minimum seam width of 12.7 mm necessitates that the overlap in the range of motion of the X/Y stages is also at least 12.7 mm. For most multiple extrusion-head FDM designs, a considerably larger overlap in stage motion will be desired. A larger overlap in stage motion allows seams to be placed at different locations on each layer. This in turn reduces the build time by allowing each extrusion head to deposit the same amount of roads even as the geometry changes. An overlap in X/Y stage motion of approximately 75 mm (3 inches) will therefore be appropriate for many applications.

4.2.4 Toolpath generating algorithm

Knowing how the perimeter and raster roads will be deposited and the shape of the seams allows for the formulation of a toolpath generating algorithm. The algorithm will be more complex for a multiple extrusion-head FDM than for a single-head FDM due to needing to avoid collisions between the extrusion heads while minimizing the required build time. The greatest time savings are realized when each extrusion head works concurrently, which in turn necessitates the equal distribution of work amongst them. This is achieved by first optimizing the placement of the geometry within the build envelope. The location of the seam between roads deposited by different extrusion heads is then calculated for each layer to allow each head to deposit as close to the same amount as possible. This will be facilitated by calculating the amount of roads that each head will deposit as a function of the placement of the part relative to the centerline. Finally, the heads will each be assigned separate build regions that can be filled simultaneously without the possibility of collision. This will be achieved by having all but one head work in the vicinity of the road overlap while the remaining head deposits roads on the extreme opposite side of the geometry.

Areas where the extrusion heads will deposit roads first will be referred to as "first build-areas" whereas the "second build-areas" are the remaining locations where the extrusion heads will deposit roads. If the first build-areas deposited near the road overlaps are at least as wide as the minimum distance that must be maintained between extrusion heads to avoid a collision, then it is possible to fill the rest of the area on the layer with a single second build-area for each head. The following flow chart (Figure 39) will serve as an outline of the procedure used to calculate toolpaths for each extrusion head in a multiple extrusion-head FDM. The toolpaths are then used to generate the numerical control (NC) code that instructs the FDM how to build a part.

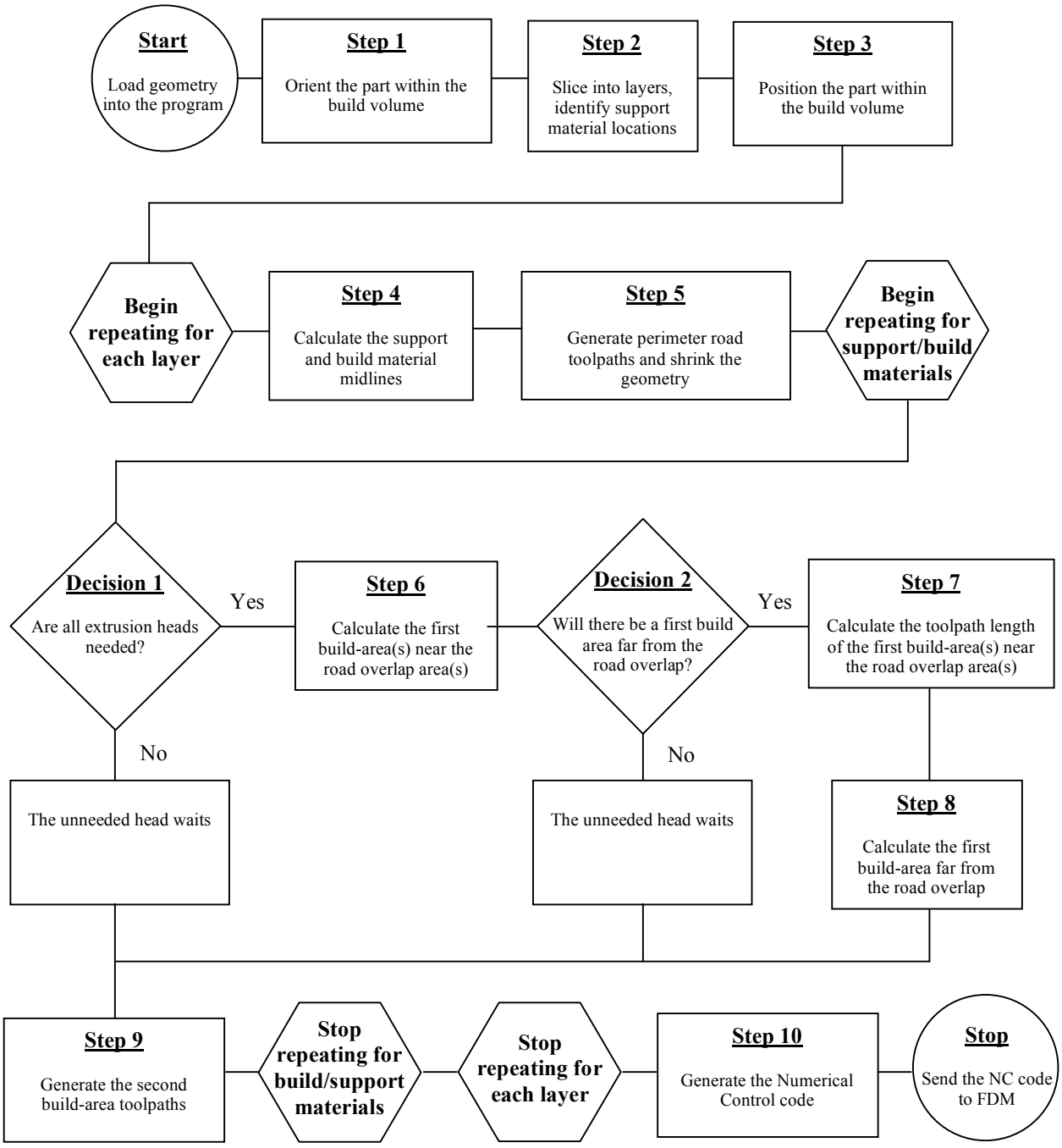

Figure 39 Flow chart showing the process used to generate toolpaths.

Step 1: Orient the part within the build volume.

Here the term "orientation" is used to refer to the rotation of the part about the X, Y, and Z axis as opposed to the absolute coordinates of the part. The original orientation of the geometry within the build volume is specified by the global coordinate-system used by the designer when creating geometry within the CAD software. Often it is desired to rotate the geometry prior to slicing into layers in order to reduce the amount of support material that is needed or to reduce the stair-stepping defect on curved surfaces. For example, consider a cylinder that is oriented to lie within the build volume so that its circular ends are vertical. Each layer would contain rectangles of material to be deposited, with the size of the rectangles increasing up to the middle of the cylinder and then decreasing again. A FDM machine cannot build in mid air, and so would require support material to be deposited under the overhangs created by the increasing rectangular cross sections. At the same time, the desired curved surface is approximated by the size of the rectangles on each layer and therefore will exhibit a pronounced stair-stepping effect unless a very thin slice thickness is used. If the cylinder was instead oriented so that it stood on a circular end with the curved surface being vertical, then the overhangs would be eliminated along with the need for support material. Also, orienting the cylinder this way would result in a smoother surface as each layer would contain circles of material that can be deposited with a high accuracy even if thick slices were used to reduce the build time.

It becomes even more important to orient the build geometry when multiple extrusion-heads are used. This is because the aspect ratio of the geometry also becomes important. An intuitive understanding can be reached by considering the case of a rectangular block with a width approximately equal to the minimum distance between heads to prevent a collision, and a length many times that width. If the block is oriented so that its length is parallel to the centerline, then each layer will be deposited by only one head at a time because there will not be enough room for both extrusion heads to deposit roads without possibly colliding (Figure 40). Alternatively, if the length is

perpendicular to the X/Y stage overlap, then there will be plenty of room for both heads to deposit roads simultaneously.

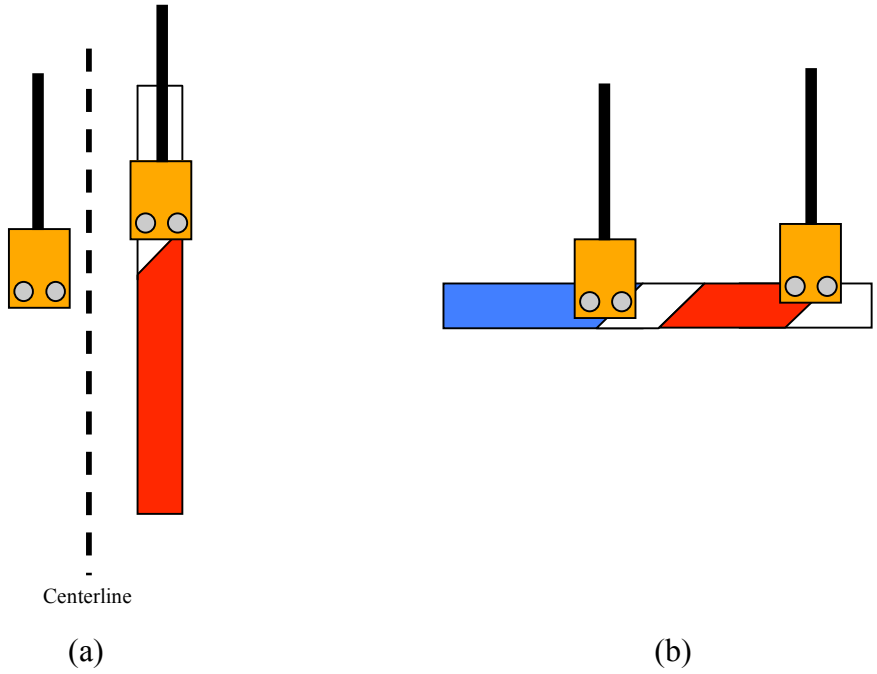

Figure 40 (a) When the block is oriented with its length parallel to the centerline, then only one extrusion head can deposit roads at a time. (b) Rotating the part 90° allows both extrusion heads to work simultaneously.

It is possible to imagine a computer algorithm that would be capable of orienting the geometry within the build volume so as to achieve a compromise between needing few supports, producing high quality surfaces, promoting thick layer slices, and allowing both heads to operate simultaneously. However, different operators would likely place different amounts of emphasis on each of the afore-mentioned factors. This would lead to a disagreement with the algorithm for some parts. It would thus be best to allow the operator to have the final say in deciding the orientation of the part within the build volume.

Step 2: Slice the part and identify support material locations.

This is a simple yet important step that is a combination of two different common tasks. Commercial rapid prototyping systems typically slice the geometry into two-dimensional layers that, when stacked on each other approximate the desired part. It is also very common to use computer algorithms to compare adjacent slices to identify overhangs and to automatically generate supports. In a multiple independent extrusion head FDM scheme the software would handle these tasks in the same way that they are currently addressed.

Step 3: Position the part within the build volume.

Commercially available FDM software allows the user to position build geometries within the build volume at any location that the operator desires. This has the advantage of allowing the operator to position the part over unused areas of the base material (the base material is an easily damaged foam in older modelers, whereas newer machines use a plastic tray). In a single-head system it does not matter where the build is located within the build volume, whereas in a multiple-head system the time required to build a part will be strongly influenced by how much material is deposited by each head. It is therefore critical to calculate the optimum placement of the geometry within the build volume so that the build time is as low as possible and the maximum benefit of using a multiple-head system is achieved.

The amount of time needed to build an arbitrary part is the sum of the time needed to build each layer, which is in turn just the longest time required for a head to deposit all of its roads. The reason why only the longest time is important is because the other heads can finish depositing all of their roads while the head that requires the most time is depositing its roads, provided that they all deposit roads simultaneously. For example, suppose that a layer requiring 48 minutes to deposit is fabricated by a two-head system. If one head requires 3 minutes to deposit its roads and the other head requires 45 minutes,

then the time needed to build that layer will be 45 minutes because the quick head must wait for 42 minutes while the slower head finishes depositing all of its roads.

The amount of time that an extrusion head requires to fill an area can be roughly approximated as being directly proportional to the size of the area. This implies that the best strategy to minimize the build time is to ensure that each head deposits the same area of roads on each layer. Consider the effect that changing the position of the part in the above example would have. If the part was positioned so that each head deposited the same amount of roads on that layer, then they would each require 48 minutes/2 = 24 minutes to deposit their roads and would both finish at the same time instead of one head having to wait. This would reduce the build time for that layer from 45 minutes to 24. The optimum positioning of a symmetrical part (e.g., a cube or cylinder) would thus have an equal amount of volume on each side of the centerline.

While each layer of symmetrical shapes will always have an equal amount of area on either side of the centerline, parts that are asymmetric will often need to be positioned differently to achieve the lowest possible build time. This is because dividing up the build area evenly on one layer may cause other layers to have a large discrepancy in the time each head requires. For example, consider a part that is ramp shaped. If the part is placed with the bottom layer having equal areas on both sides of the centerline, then the top few layers may be only accessible by one head, forcing the other to wait inefficiently. Although the exact location of the seam can be adjusted from one layer to the next so long as it remains within the overlap in X/Y stage motion (so that both heads can reach all locations where they need to deposit roads), most parts will have dimensions that are much larger than the X/Y stage overlap width. Thus the location of the part within the build volume that results in the lowest possible build time will need to be calculated during this step and then in Step 4 the location of the seams within the X/Y stage overlap region will be determined on a layer by layer basis. While determining the optimum placement of the part within the build volume, all the area on one side of the centerline will be considered to be built by the same head even though the seam will really be at a 45° angle with respect to the centerline. This is because from geometrical arguments it

can be proven that the areas in both cases are equivalent but the straight line is easier to visualize and simplifies calculations. The basic strategy therefore consists of predicting the build time as a function of the placement of the part relative to the centerline. This is accomplished by varying the location of the part while recording the total build time needed and then examining the record to find the position with the smallest build time.

As stated above, it will be assumed that filling an area with roads requires an amount of time directly proportional to the size of the area. The task at hand then becomes to calculate the area on each side of the centerline for each layer. One way to achieve this is via integration of the lines that describe the solid/air interface. The area under a curve is merely the integral of the curve with limits of integration equal to the edges of the area. After slicing into layers in the previous step, the solid/air interface is represented by many little discontinuous straight line segments, the equations for which are in the form:

$$Y = mX + b \quad \text{over the interval } X = A \text{ to } X = B \qquad \text{Equation 8}$$

The area is simply the integral of the top curve minus the integral of the bottom curve [Stewart 1995]. In this case, the line segments can be divided into top line segments and bottom segments by looking at the interval over which they are found. Vertical line segments are ignored since they do not contribute any area. Out of the two line segments that have the lowest X-coordinate endpoints, one segment will usually have a positive slope and therefore belong to the top curve while the other has a negative slope and belongs to the bottom curve. The exception is the case when one or both of the lines are horizontal. In this case the lines must have been connected by a vertical segment and determining which curve they belong to is as simple as looking at the Y-coordinate of their start point. Segments that share the same endpoints as these line segments are then appropriately added to either the top or bottom curve. The process of adding line segments to the top or bottom curve is continued until the segments with the largest X-coordinate endpoints are used. In the case of complex parts with hollow regions, the process must be repeated for each of those regions and then the area of those regions

removed from the total area. Because the equation that describes the top and bottom curves is discontinuous, the integrals must be broken up into multiple integrals, each acting on a function that is continuous over the limits of integration.

$$\int_A^Z \text{discontinuous function} =$$

$$\int_A^B \text{Function continuous from A to B} + \int_B^C \text{Function continuous from B to C} + \int_C^D \text{Function continuous from C to D} + \ldots$$

Equation 9

There will therefore be one integral for each line segment that is not vertical. At first this seems daunting, but all of the line segments are straight lines and their integration is simply:

$$\int (mX + b)\,dX = \frac{m}{2}X^2 + bX + c \qquad \text{Equation 10}$$

Where the integrating constant, *c*, is zero in this case. Thus the computational expense is low as finding the area involves simply separating the line segments into curves and then evaluating $mX^2/2 + bX$ over the domain of the line segment using the same values for *m* and *b* as in the original equation that describes the line segment. If the line segment was in the top curve then the result is added and if the line segment was in the bottom curve the result is subtracted. The resulting summation is the area.

Alternatively, the areas can be found graphically by placing the desired geometry of a layer onto a grid composed of squares with sides the same length as the width of a road. The number of squares that contain any build or support material are then simply counted. A constraint is added that one of the grid lines should always lie on the centerline so that fractional squares need not be counted.

While it may appear to be a poor approximation of small geometries (as in the case of the circle shown in Figure 41), larger build geometries will have a lower

percentage of error. The fact that the squares' dimensions are equal to the road width, and that the stepper motors have a minimal move distance, will cause the extrusion head to spend significant time in any square that contains even a small amount of perimeter. This makes the actual error less than would be perceived from the illustration. Also, the percentage of error caused by including a square that contains only a small amount of perimeter is small. This is because moving the part to an adjacent location typically changes the number of squares that each head will deposit by at dozens of squares.

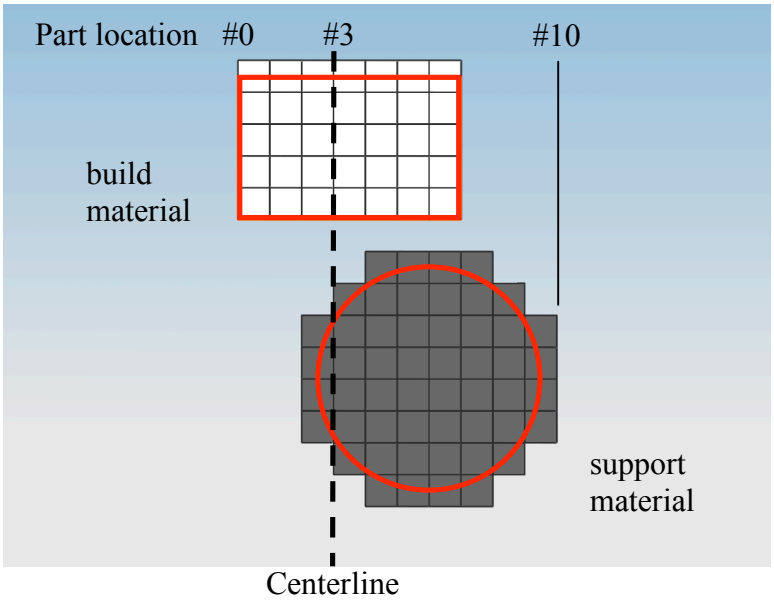

Figure 41 Illustration of the grid used to count the area build by each head. When the part is at location #3, then the left head will deposit 15 squares of build material and 4 of support material. The right head will deposit 20 squares of build material and 48 of support material.

Determining the optimum placement of the part within the build volume requires first placing the part at location #0, so that all the area is to the right of the centerline. The area that each head would need to deposit support material is calculated for the first layer (either integration or rectangle counting can be used). The larger number is then stored in a matrix called the "support matrix." The area that each head would deposit

build material on the first layer is then calculated and the larger one is also stored in a matrix called the "build matrix." A third matrix, the "total matrix," stores the sum of the larger of the build areas plus the larger of the support areas (Table 5). The sum of the two larger values represents the total time needed to fabricate that layer. The smaller areas are discarded because they do not contribute to the build time. The simultaneous movement of the extrusion heads allows the smaller build-area to be completed while the larger build-area is being laid down. This process is repeated up to the top layer, with the information for each layer recorded in a different row of the same column. The location of the part relative to the centerline is incremented by some small amount (such as the width of a road), and the area calculations for each layer are repeated, with the values being recorded in a different column of the matrix. The entire process of moving the part relative to the centerline and calculating and then storing the areas is repeated until all the area is to the left of the centerline. This will result in three matrices, each with the same number rows as there are build layers. The "total matrix" will be used immediately for the determination of the optimum placement of the part while the "build matrix" and "support matrix" are saved for use later. Someone familiar with matrix math may note that it is possible to combine these three matrices into one matrix that is three times as large. However, for the sake of clarity and simplicity the distinction between the matrices, each containing a different type of data, will continue to be made.

Table 5 Example of the areas calculated by counting rectangles in Figure 41. The highlighted values are stored in the matricies. Units = (road width)^2

Part location #	0	1	2	3	4	5	6	7	8	9	10
Left head support	0	0	0	4	10	18	26	34	42	48	52
Right head support	52	52	52	48	42	34	26	18	10	4	0
Left head build	0	5	10	15	20	25	30	35	35	35	35
Right head build	35	30	25	20	15	10	5	0	0	0	0
"support matrix" row	52	52	52	48	42	34	26	34	42	48	52
"build matrix" row	35	30	25	20	20	25	30	35	35	35	35
"total matrix" row	87	82	77	68	62	59	56	69	77	83	87

With the calculation of the areas complete, the total matrix will have one row for each layer, and a column for each different possible position. Each column is then summed to determine the total build time required to fabricate the desired geometry if the part was located at that position. The position with the lowest build time is the one that is then used. In the example shown in Figure 41 and Table 5, the optimal position would be location #6 (circled).

A multiple extrusion-head system with both more than one column and more than one row of extrusion heads must have the part positioned in both the X and Y directions. The procedure is adapted by calculating the optimum location in one direction at a time by combining the computed areas in the build volumes of all the extrusion heads in the other direction. For example, consider a FDM with two extrusion heads in the X direction and three in the Y direction (Figure 42). When the position of the part is calculated in the X direction, the areas that would be built by extrusion heads 1, 3, and 5 are added together and so are the areas of heads 2, 4, and 6. This results in simplifying the build volume to resemble a two-head system. Similarly, when the position of the part in the Y direction is calculated, the build volumes of heads 1 and 2 are combined, 3 and 4 are combined, and 5 and 6 are combined. This results in a case that is the same as when 3 extrusion heads are used. Once the optimum placements for both directions are calculated, the computer model of the build geometry is placed at the corresponding location.

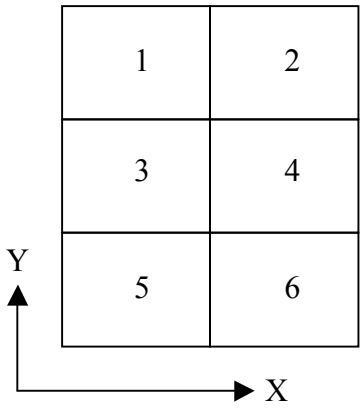

Figure 42 A multiple head FDM system with 2 stages in the X direction and 3 in the Y direction

Step 4: Calculate the build and support midlines for each layer.

The midline is defined as a straight line that is parallel to the centerline, and simply stands in for the more complex seam (Figure 22). This reduces calculation complexity without modifying the amount of area built by the extrusion heads since they areas are geometrically equal in both cases. In a later step the seam in the support material will replace the support material midline and the seam in the build material will replace the build material midline. The locations of these midlines do not need to coincide, and so the build and support material midlines will often be located at different positions.

The property of 45° seams that they are able to be translated perpendicularly to the centerline (Section 4.2.3), can be used to further reduce the build time. By adjusting the locations of the seams, the difference in the amount of area built by each extrusion head can be reduced. This is accomplished by first removing the columns from the build matrix and support matrix that correspond to positions that cannot be reached by both extrusion heads. The width of the seam is subtracted from the width of the overlap in X/Y stage motion, and the result is then divided by two. Any midline located at cells corresponding to a position farther from the centerline than this distance will contain road

coordinates that cannot be reached by both extrusion heads. The reason why the width of the seam must be subtracted is because the seam will extend past both sides of the location of the midline by half of its width. The lowest value in the remaining cells of the support matrix becomes the midline location for the support material and the lowest value in the build matrix becomes the location of the midline for the build material. For example, consider again the case of Figure 41 and the corresponding matrix data presented in Table 5: If the part is positioned so that it is at location #6 and locations 4 through 8 are valid locations for midlines, then the support material midline would be located at #6 and the build material midline would be located at #4 (enclosed by squares in Table 5). The total build time is then reduced from 56 time units (the units are equal to the road width / the length of road deposited per second) to 46 time units. Compared to the time required for a single extrusion head FDM to build the layer (87 time units), this is a significant reduction in build time.

Step 5: Generate the perimeter toolpaths and shrink the geometry.

This step aims to generate the toolpaths that will deposit the perimeter roads and then remove the area occupied by them from the geometry so that the raster fill fits correctly. It is typically assumed that the user desires the perimeter to be deposited on the same line segments that define the air/solid interface only offset inwards by half the road width so that the outside of the perimeter roads coincides with the location of the interface. This involves scaling the vectors that describe the air/solid interface. Once the line segments have been scaled, they are stored in the computer's memory for use as the toolpath that will deposit perimeter roads. Start and end points will need to be located where the seam intersects the perimeter toolpath during Step 6 (below) for the appropriate extrusion heads.

With the toolpath saved in memory, the line segments must be further offset inwards by another road width so that they can be used to represent the farthest outwards location of the raster roads without a collision with the perimeter roads. The reason for

the line segments to be offset inwards by another road width is that the perimeter roads will lie with half their width inwards while the raster pattern roads placed on the inwards offset line segments will also have half their width lying towards the outside. Very small features with a thickness less than three road widths will result in areas that are too narrow for any raster pattern roads to fit inside. Algorithms commonly search for such areas and remove them. Once the line segments have been offset inwards, scaled down, and any areas too small for roads to fit inside removed, then the resulting line segments can be used to define the outermost placement of the raster pattern roads. As such, the boundary formed by all the line segments shall be referred to as the "raster boundary."

Decision 1: Are all the extrusion heads needed?

This check involves little more than examining the domains of the equations that describe the air/solid interface. If at least one line segment passes through the build volume of an extrusion head, then that head will need to fabricate a portion of the geometry on that later. Conversely, if no geometry lies within the build volume of an extrusion head, then no boundary between the air and solid can lie within the build volume.

Step 6: Calculate the first build-area(s) near the road-overlap area(s).

The procedure for calculating the first build-area near the road overlap in a two-head system is to first replace the midline with the seam. The seam should alternate from one layer to the next, between +45° and -45° relative to the centerline. The width of the build area should be equal to the minimum distance required to prevent any possibility of a collision between the two heads, plus a small amount extra (~0.2 mm) to provide a margin of safety. It is important that the width of the first build-area is an even multiple of the road width. This allows for a continuous toolpath to be possible, the reasons for which shall be shown shortly. Next, a second seam is added, this time offset in the

negative X direction from the midline location by a distance equal to the desired first build-area width. It is important to note that the second seam has the same shape as the first one and is offset in only the X direction. The enclosed area between the two seams and the raster boundary is then the first build-area for the extrusion head near the road-overlap area.

The same steps are implemented in systems with more than two heads, but there will be one first build-area near each road-overlap area. For example, a three head FDM would have two road-overlap areas, and therefore would have two first build-areas to be determined in this step. In the case where there is more than one row and more than one column of X/Y stages, then the road-overlap areas necessitate first build-areas along the X direction and the Y direction (Figure 43).

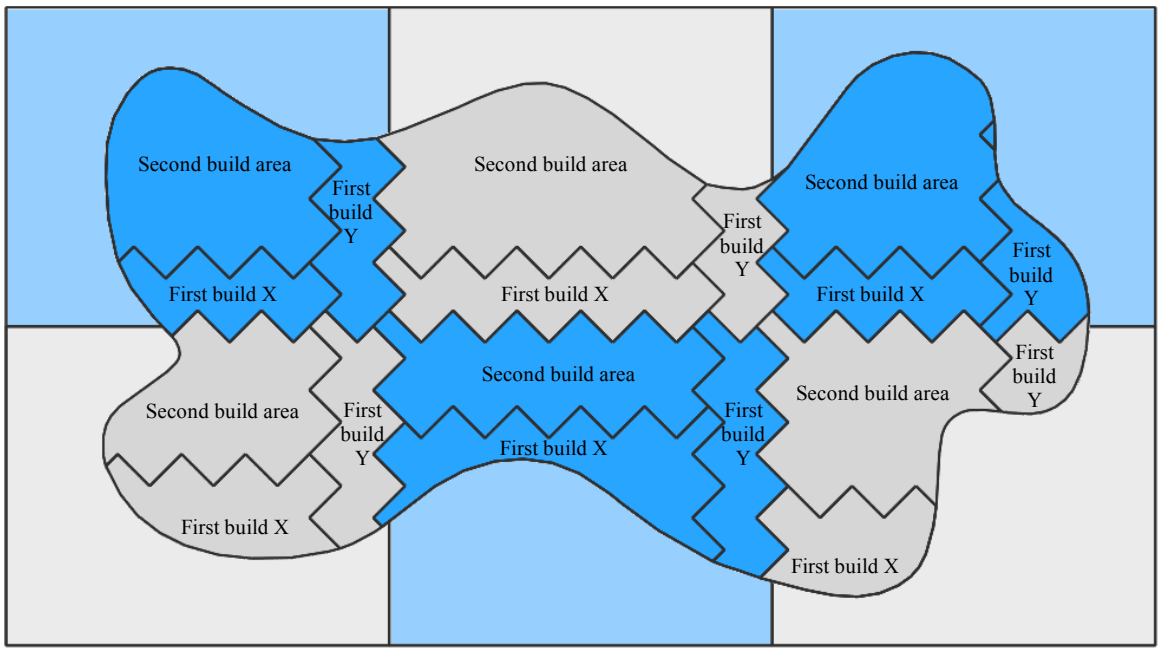

Figure 43 Arbitrary shape built by a 6 extrusion head machine with 3 X/Y stages in a row. Each extrusion head has a first build-area in the X direction, a first build-area in the Y direction, and a second build-area.

Decision 2: Will there be a first build-area far from the road overlap?

While roads are being deposited within the first build-area near the road overlap, the remaining extrusion head should deposit roads far from the road overlap. However, some geometries may lack sufficient size for roads to be deposited in both areas while maintaining sufficient separation between the extrusion heads to prevent a collision. Therefore a simple check should be performed to determine if the extrusion head that deposits roads far from the road overlap can have a first build-area. This check involves determining if any of the geometry lies within the build volume of the remaining extrusion head but outside of the minimum distance from the seam to prevent any possible collision with the head that is depositing roads near the road-overlap area. The build volume will contain an imaginary boundary between points that lie closer to the seam than the minimum distance to prevent a collision, and those that lie outside of it. As the minimum distance is constant, the "collision boundary" will have the same shape as the seam but will be offset in the X direction. The magnitude of the offset will be the same as the width of the first build-area near the road overlap because the same arguments of needing a margin of safety and aligning with roads apply. If there exists any region to be filled with raster roads beyond the collision boundary, then there will be a first build-area far from the road overlap, although the precise size and shape of the first build region will be determined later (Figure 44). If there is no area beyond the collision boundary, then the remaining extrusion-head will wait as roads are deposited near the road-overlap area.

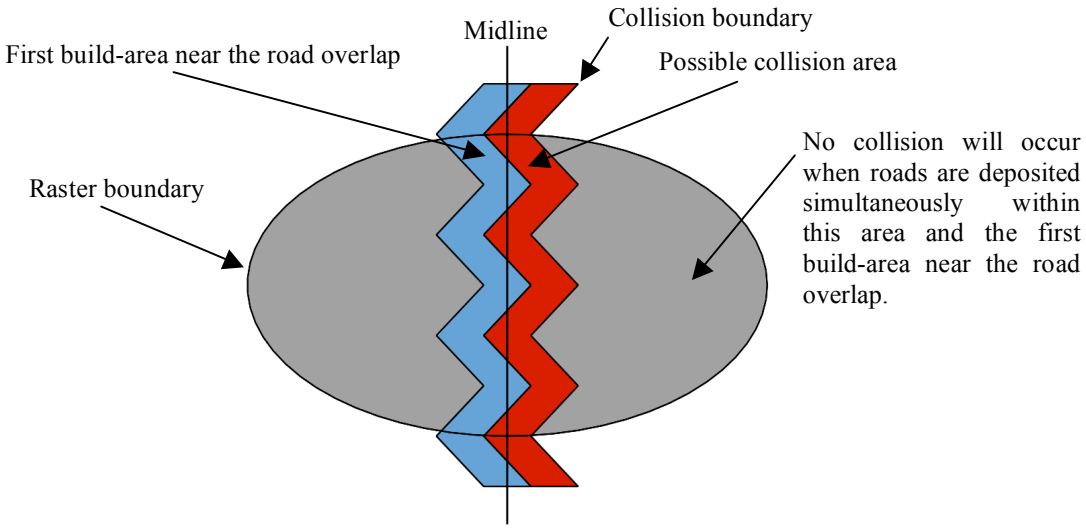

Figure 44 Illustration of an arbitrary geometry that will have a first build-area far from the road-overlap area.

Step 7: Calculate the toolpath length of the first build-area near the road-overlap area.

Both first build-areas should contain the same toolpath length so that they require the same amount of time for the roads to be deposited. Because the first build-area near the road overlap is a function of the geometry and the minimal distance to avoid a collision, it has a fixed size and cannot be changed. The first build-area far from the road overlap, on the other hand, can have a magnitude that ranges from zero to the entire area beyond the collision boundary. In order to set the toolpath length contained within the two first build-areas to be equal, the length of roads that will be deposited in the first build-area near the road overlap must be calculated. This necessitates knowing the toolpath. The toolpath is determined by first intersecting the geometry with dexels (infinitely long rays with zero diameter) at +45° for one layer and then -45° on the next layer. While the dexels have no diameter (they are infitesimally thin), the spacing of the dexels is the same as the road width. The seams and the dexels should line up with one another so that the dexels can be used for toolpath generation. In the case of a fast build part, the sparse

interior structure is generated by changing the dexel spacing to be three or four times the road width. This causes the roads to be deposited with space equal to two or three times the road width between them.

After dexels are intersected with the geometry, a location for the start point of the road is selected. Either the highest-leftmost intersection between a dexel, the seam, and the raster boundary or the lowest-rightmost intersection between them should be used. The toolpath for depositing the road then follows the dexel into the first build-area until it reaches a seam or a raster boundary that is perpendicular to the dexel. A short line segment is then added to connect it to the next dexel over and the toolpath then follows that dexel (Figure 45). The line segment should connect the intersection of the dexel with the seam/raster boundary with the intersection that the adjacent dexel makes with the same seam/raster boundary. This results in the curvature present in a curved raster boundary to be simplified into a straight line segment that the X/Y stages can follow. This process is continued until no more dexels can be reached without crossing a seam or raster boundary. The last intersection that can be reached is the endpoint of the road. In the case of a simple toolpath all dexels within the first build-area will be used and the entire first build-area will be accounted for. A complex toolpath will still have unused dexels within the first build-area, and will necessitate creating additional start points, each new start point being the next highest-leftmost / lowest-rightmost intersection. A straight line segment is added to connect the first end point to the second start point, the second end point to the third start point, and so on. Although no material will be deposited as the head follows these connecting line segments, the extrusion head will still need to move from the first endpoint to the second start point. The toolpath is saved for latter and the length of each line contained within the toolpath is calculated and summed (including the dexel segments). This total length is the sought after road length the first build-area near the road overlap.

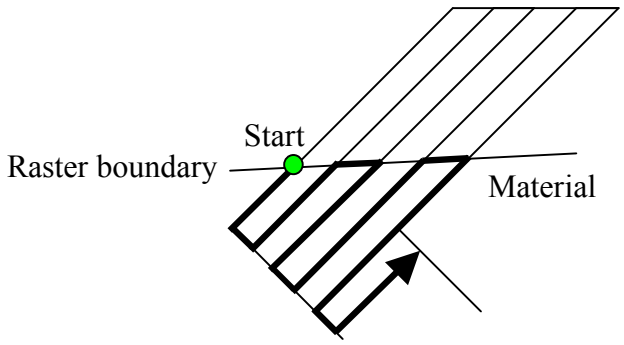

Figure 45 Toolpath generation using the highest-leftmost intersection for the start point.

It is now possible to see why the width of the first build-area needs to be an even multiple of the road width. As the toolpath follows a dexel it will turn around and change directions once it reaches a raster boundary or seam. Therefore, it will reverse directions once per each dexel, and the number of dexels equals the number of road widths as the spacing between dexels is equal to the width of a road. An even multiple of road widths will thus result in the raster roads changing directions an even number of times for each time that the seam changes directions. By changing directions an even number of times, the roads will travel in the same direction that they traveled the previous time that the seam was at the same angle (Figure 46.a). This in turn prevents a complex toolpath from being formed each time that the seam is perpendicular to the dexels (Figure 46.b).

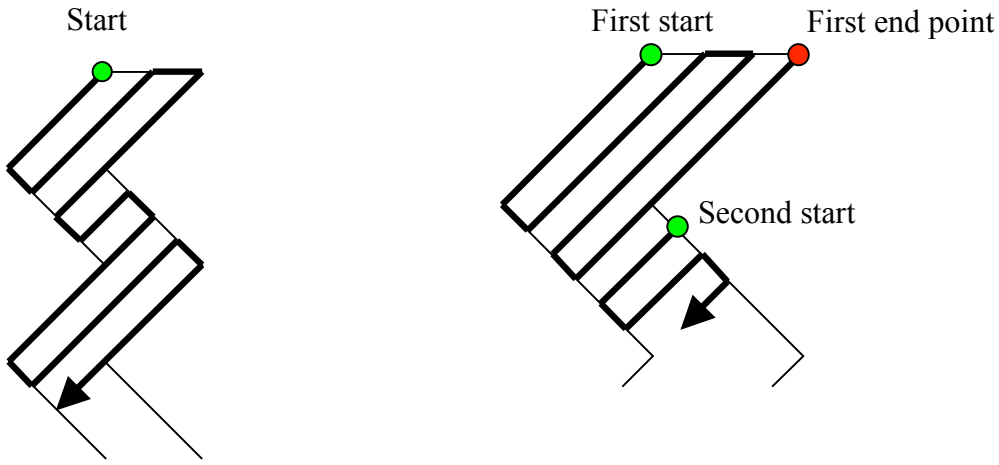

Figure 46 (a) Simple toolpath resulting from the first build-area's width being an even multiple of the road width. (b) The complex case that arises when the width is an odd multiple of the road width.

Step 8: Calculate the toolpath for the first build-area far from the road overlap.

With the desired toolpath length calculated in Step 7, it is now possible to calculate the size of the first build-area far from the road overlap, as well as the toolpath. The first build-area will be the enclosed area between the raster boundary line segments located farthest from the centerline and a seam. As has been the case with the previous seams, this one should also align with the dexels. Initially the seam should be located at the collision boundary; although it may need to be moved latter. A start point is then chosen at the highest-leftmost / lowest-rightmost intersection between the raster boundary, dexel, and seam line segments. The toolpath then follows the dexel into the area to be filled with raster roads until a raster boundary or perpendicular seam line is encountered, at which time a short line segment is added to connect the toolpath to the next dexel over. As was seen previously, if the toolpath is simple then the entire area will be accounted for while the complex case requires that the endpoints are connected to the next start point until all the area is filled.

The total length of the toolpath is then calculated and temporarily stored in computer memory along with the corresponding location of the seam relative to the centerline. If the toolpath length is less than the toolpath length of the first build-area near the road overlap, then the calculation of the first build-area far from the road overlap is complete since there is no way to increase the size of the first build-area beyond its initial size, which encompasses all of the area beyond the collision boundary. However if the toolpath length is greater than that of the first build-area near the road overlap, then the seam is moved away from the centerline by half of the distance to the farthest raster boundary line segment (rounded to lie on the nearest dexel) and the calculation is repeated. If subsequent calculations of the toolpath length yield a length that is less than the toolpath length of the first build-area near the road overlap, then the location of the seam is moved back towards the centerline by half the distance between the previous and current locations (again rounded to the nearest dexel location). After the first time that the seam is moved towards the centerline, it will only be moved back away from it by half the distance to the previous farthest seam location. The process of interval halving continues until the toolpath lengths are as close as possible to being equal to each other. Note that the constraint that the seam must lay on a dexel causes the minimum distance that the seam can be moved to be the distance between dexels, which in turn limits the number of times that the calculation can be repeated before the seam is merely jumping back and fourth between two adjacent locations. This provides the condition to stop calculating when the next seam location is the same as a previous location. Out of those two adjacent seam locations, the one that makes the toolpath lengths as close to one another as possible is selected for the final seam location (Figure 47).

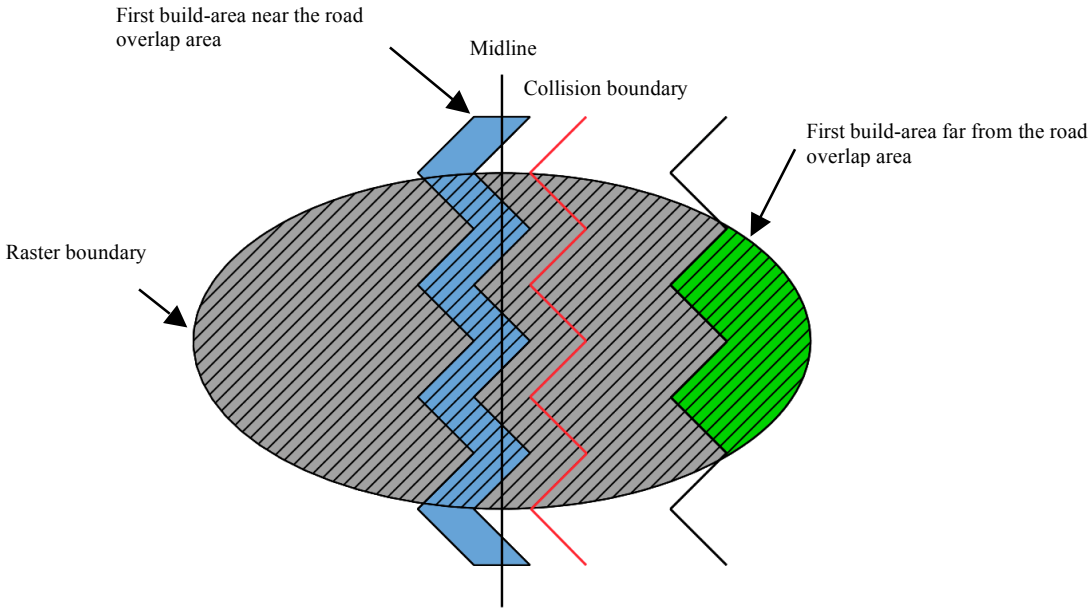

Figure 47 The first build-area far from the road-overlap area (shaded green) is calculated for an arbitrary shape. The length of the toolpath is the same as the first build-area near the road overlap (shaded blue). The remaining second build-areas (shaded grey) also contain equal road lengths.

Step 9: Generate the second build-area toolpaths.

If either of the decision steps in Figure 39 have been evaluated to have a "yes" answer, then at least one toolpath for a first build-area will already exist, along with the dexels that were intersected with the geometry. The toolpaths for the second build-area(s) are then generated in this step. Alternatively, if both decisions were "no," then dexels will need to be intersected with the geometry at this time. In this step toolpaths are generated for all of the areas to be filled with the raster pattern that were not filled by a first build-area. The toolpath generation procedure used in this step is the same as the procedure used to generate toolpaths for the first build-areas.

Step 10: Generate the numerical control code.

In this step all of the toolpaths for the current layer will be compiled into a single set of numerical control commands that direct the FDM machine. The commands should instruct the FDM to first deposit the perimeter roads (Step 5) so that the surface of the part can be accurately represented without defects that may be introduced due to interactions between the perimeter road and raster pattern. The FDM next deposits the first build-areas (Steps 7 and 8) followed by the second build-areas.

Pauses should be added to the NC code in this step so that the heads wait when needed (such as when only one head is depositing roads or when the Z stage moves). Starting or stopping a road will not require the heads to pause to allow movement of the Z stage. As discussed in Chapter 3, each nozzle will have a solenoid so that it can be moved upwards to terminate the road without the Z stage moving down. The nozzles will also be raised to prevent a collision when the extrusion head needs to pass over an existing road. Commands are inserted into the NC code at the location of start/stop points to instruct the stepper motors within the extrusion heads to feed material into the extruders to deposit roads or to draw some material back to terminate the road. Once the NC code is generated for each layer, the instructions are ready to be sent to the FDM for fabrication of the part. Sending the NC instructions to the FDM is the last task required of the software, and completes the toolpath generation process.

Chapter 5

Conclusions

In this final chapter the previous chapters are summarized. A list of contributions by the author is then presented.

5.1 Summary

This work has illustrated the fundamental workings of a multiple independent extrusion-head FDM. With such a machine it is possible to realize significant time savings which, when used in combination with other time saving techniques, should greatly advance the possibility of using rapid prototyping machines for tool-less manufacturing. Utilizing multiple extrusion heads is also one method for increasing the build volume without increasing the amount of time required for fabricating parts. Due to the partitioning of the part's geometry and the simultaneous deposition of roads by the extrusion heads, the time needed to build an arbitrarily large part can be reduced to the time that just one extrusion head requires.

Collisions between the extrusion heads must be avoided or else the impact will cause their locations to be different than expected. This in turn will result in the deposition of all subsequent roads in the wrong place, which would ruin the part being built. A minimal distance will therefore be maintained between the extrusion heads so that there is no possibility of a collision. The extrusion heads can be redesigned to reduce the minimum distance by repositioning components within the extrusion heads, making the extruders vertical, and adding a fillet to the corners of the extrusion heads. Solenoids should be added to the build nozzles so that they can be raised up without moving the Z stage. This allows extrusion heads to continue working at times when they would

otherwise need to wait while the Z stage is actuated to terminate a road, or to allow an extrusion head to pass over previously deposited roads

Any number of extrusion heads can be used in a multiple-head machine so long as either vertical feeding tubes are used, or no X/Y stage is surrounded on all sides by other stages. This is due to the interference caused by horizontal feed tubes when an extrusion head is surrounded. The build and support nozzles of all extrusion heads should be at the same height so that a common Z stage can be used. The planes of motion of all extrusion heads should also be coplanar so that fabricated parts are not warped or skewed. Both of these concerns can be addressed by using adjustment screws at each corner of the X/Y stages. The extrusion heads are moved to each corner and the heights of the nozzles are made the same by measuring the distance between the Z stage and each nozzle and then adjusting the screw at that corner. A simplification can be made by using group stages that consist of several X/Y stages that use shared Y-axis guide rods. Group stages facilitate calibration of the height of the nozzles by reducing the amount of calibration that is required and by guaranteeing that the extrusion nozzles are coplanar.

There is also a need to calibrate the machine coordinate system of each X/Y stage. This is because the roads that one head deposits must align with the roads that the adjacent heads deposit. The calibration process consists of fabricating a small test box, half of which is deposited by each of two adjacent extrusion heads. The deviation of the fabricated part from the desired shape indicates the difference between the two adjacent stages' coordinate systems. Once the difference is known, the instructions to the stages can be modified to correct the difference. The calibration of a multiple extrusion-head FDM will rarely need to be performed and is not highly time consuming or difficult.

The toolpath generating algorithm presented in this work seeks to allow for the simultaneous movement of all extrusion heads without the possibility of a collision between them. This is achieved by further subdividing the areas to be built by each extrusion head into first and second build-areas. A seam occurs at the boundary between the roads deposited by different extrusion heads, or between the roads deposited by the

same extrusion head at different times. While one extrusion head deposits roads near the road overlap, the other head deposits roads far enough away that there is no possibility of a collision. The width of the first build-area deposited near the road-overlap area is chosen to be at least the minimum distance between the extrusion heads needed to prevent the possibility of a collision. Knowing its toolpath length allows the first build-area that is deposited far from the road overlap to be chosen so that it requires the same amount of time to deposit. The extrusion heads are then free to deposit all the roads in their second build-areas without the possibility of a collision.

Roads deposited by one extrusion head need to interact with the roads deposited by the other extrusion head on adjacent layers, so that forces acting on them can be transmitted across the seam. The magnitude of the road-overlap area depends on the location of the seams, and on the seam width. Seams separated by some distance will produce a greater road-overlap area while seams located at the same place will produce a minimal road-overlap area. Tensile tests have shown that when the seams are located at the same location, a seam width greater than 13 mm (0.5 inches) is sufficient to produce parts with comparable mechanical properties as parts fabricated by a single extrusion head.

A simple algorithm can be used to determine the optimum placement of the part within the build volume. This allows the difference in the size of the areas that the extrusion heads deposit to be minimized. The amount of area that each head would deposit on each layer as a function of the position of the part relative to the centerline is calculated by either integrating the line segments that indicate the air/surface boundary, or by counting squares in a grid. The time needed to build each layer is then summed to find the total amount of time required to fabricate the part at each possible position. The optimum position of the part can then be identified. Because some parts may be anti-symmetrical or slanted, there may be layers containing differences in the amount of area that each extrusion head is responsible for. A compensation for the differences can be made by changing the location of the seam on a layer-by-layer basis to any position

within the overlap in X/Y stage motion. This further equalizes the areas and reduces the build time.

The perimeter roads should be deposited before the internal roads so that their shape is not distorted by interactions with the internal roads. The line segments that define the boundary between air and solid material can be scaled down in size to compensate for the road width. They are then used for the toolpaths to deposit the perimeter roads. Extra start and stop points must be added so that the extrusion heads can each deposit the perimeter road segments that fall within their build volume. These extra start and stop points are barely noticeable in fabricated parts and do not significantly detract from the surface finish. After the perimeter roads have been deposited, the internal roads are deposited in the first build-areas and then in the second build-areas. These internal roads should be deposited using a raster pattern that alternates from one layer to the next between +45° and -45° relative to the centerline.

Once the toolpaths have been generated, additional instructions are added to control the Z stage and extruders. The instructions for each layer are then compiled into a single set of numerical control commands that are then ready to be sent to the FDM machine.

5.2 Original Contributions

The author regards the following as original contributions in this work.

- A method to calibrate multiple X/Y stage machines. It is critical in a multiple extrusion head Fused Deposition Modeler that the roads deposited by different extrusion heads align and lie in the same plane.

- Proposed group stages that employ a single set of guide rods that are shared by multiple X/Y stages. In a multiple extrusion-head FDM, a group stage has the advantages of being easily made coplanar, and being capable of producing overlapping motion in its constituent X/Y stages.

- An algorithm that determines the optimum placement of a part to be fabricated within the build volume so as to minimize the build time.

- Determining the raster pattern and seam that should be used by a multiple extrusion-head system to promote build speed and part strength.

- A strategy that allows simultaneous extrusion-head motion while preventing the possibility of a collision.

- Determining the effect of seam width on mechanical properties of a fabricated part.

References

[3D Systems 2005] http://www.3dsystems.com
Downloaded November, 2005

[ARC 2006] (Auto Research Center)
http://www.autoresearchcenter.com
Downloaded September, 2006

[ASTM] American Society of Testing and Measurements standard D 638-03

[Baird 1998] Baird, D. G., and Collias, D. I., *Polymer Processing Principles and Design*, John Wiley & Sons, Inc., New York, USA, 1998

[Beaman 1997] Beaman, J. J., Barlow, J. W., Bourell, D. L., Crawford, R. H., Marcus, H. L., and McAlea, K. P., *Solid Freeform Fabrication: A New Direction in Manufacturing with Research and Applications in Thermal Laser Processing*, Kluwer Academic Publishers, Massachusetts, USA, 1997, pp. 1-5

[Beer 1992] Beer, F. P., and Johnston, E. R. Jr., *Mechanics of Materials, Second Edition*, McGraw-Hill Inc, New York, USA, 1992

[Beer 1996] Beer, F. P., and Johnston, E. R. Jr., *Vector Mechanics for Engineers, Sixth Edition*, McGraw-Hill Inc, New York, 1996

[Bellini 2003] Bellini, A., and Güçeri, S., "Mechanical characterization of parts fabricated using fused deposition modeling," *Rapid Prototyping Journal*, vol. 9, no. 4, 2003, pp. 252-264

[Bennett 1995] Bennett, G. (ed.), *Rapid Prototyping and Tooling Research*, Mechanical Engineering Publications Limited, Suffolk, UK, 1995, forward by Bennett

[Blanther 1892] Blanther, J. E., U.S. Patent 473,901, 1892

[CERAM 2006] CERAM Research Ltd., "Rapid Prototyping – Laser Fusion and Selective Laser Sintering," *AZojomo Journal of Materials Online*, available at:
http://www.azom.com/details. asp?ArticleID=1648

[Chen 2004] Chen, Z., Li, D., Lu, B., Tang, Y., Sun, M., and Wang, Z., "Fabrication of artificial bioactive bone using rapid prototyping," *Rapid Prototyping Journal*, vol. 10, no. 5, 2004, pp. 327-333

[Cyon 2006] Cyon Research Co., "A rapid prototyping primer Part 3: fused deposition modeling," *CADCAM Net* (www.cadcamnet.com), 2006

[da Rosa 2004] da Rosa, E. L. S., Oleskovicz, C. F., and Aragão, B. N., "Rapid Prototyping in Maxillofacial Surgery and Traumatology: case report," *Brazilian Dental Journal*, vol. 15, no. 3, 2004, pp. 243-247

[de Beer 2005] de Beer, D. F., Truscott, M., Booysen, G. F., and van der Walt, F. G., "Rapid manufacture of patient-specific shielding masks, using RP in parallel with metal spraying," *Rapid Prototyping Journal*, vol. 11, no. 5, 2005, pp. 298-303

[eFunda 2005] http://www.efunda.com/processes/rapid_prototyping /lom.cfm
Downloaded November, 2005

[Elkins 1997] Elkins, K., Janak, C., and Nordby, H., "Model Specific, Fused Deposition Modeling Using Soft Thermoplastics" M.Eng. project, Virginia Polytechnic Institute and State University, Blacksburg Virginia, USA, 1997

[Elliott 2004] Elliott, L. "Rapid Manufacture Ramps Up," *Desktop Engineering Magazine*, November 2004

[Fountaim 1994] Fountaim, T.J., *Parallel computing principles and practice*, Cambridge University Press, New York, USA, 1994, pp. 1-28

[Grama 2003] Grama, A., Gupta, A, Karypis, G., and Kumar, V., *Introduction to Parallel Computing, Second Edition*, Addison-Wesley, Essex, England, 2003, pp. 1-8

[Griffin 2004] Griffin, A., "Design Issues: Ceramic Rapid Prototyping Options," Lone Peak Engineering, Inc. (DBA Javelin 3D) presented at MD&M, 2004, available at: www.javelin3d.com/pdf/awards/CeramicRP.pdf

[Halloran 1999] Halloran, J. W., "Free Form Fabrication of Ceramics," *Engineering with Ceramics, British Ceramic Proceedings no.59*, Lee and Derby eds., 1999, pp. 17-26

[Hilton 2000] Hilton, P. D. (ed.), and Jacobs, P. F. (ed.), *Rapid Tooling: Technologies and Industrial Applications*, Marcel Dekker Inc., New York, New York, 2000

[Hopkinson 2006] Hoplinson, N (ed.), Hague, R. J. M. (ed.), and Dickens, P. M. (ed.), *Rapid Manufacturing An Industrial Revolution for the Digital Age*, John Wiley & Sons LTD, West Sussex, England, 2006, p. 2,5

[Jacobs 1996] Jacobs, P. F., *Stereolithography and Other RP&M Technologies: from Rapid Prototyping to Rapid Tooling*, Society of Manufacturing Engineers, Dearborn, Michigan, 1996, pp. 21-24

[Jamieson 1995] Jamison, R., and Hacker, H, "Direct slicing of CAD models for rapid prototyping," *Rapid Prototyping Journal*, vol. 1, no. 2, 1995, pp. 4-12

[Kai 1997] Kai, C. C., and Fai, L. K., *Rapid Prototyping: Principles & Applications in manufacturing,* John Wiley & Sons Pte Ltd, Singapore, 1997

[Kamrani 2006] Kamrani, A., and Nasr, E. A., *Rapid Prototyping Theory and Practice*, Springer, New York, USA, 2006, p. v,viii

[Kontoghiorghes 2006] Kontoghiorghes, E. J. (ed.), *Handbook of Parallel Computing and Statistics*, Chapman & Hall/CRC, Florida, USA, 2006, p. 18

[Lind 2003] Lind, J-E, Hanninen, J., Kotila, J., Nyrhila, O., and Syvanen, T., "Rapid Manufacturing with Direct Metal Laser Sintering," *Materials Research Society Symposium Proceedings*, vol. 758, Material Research Society, Boston, USA, 2003, pp. 17-22

[Masood 2005] Masood, S. H., and Song, W. Q., "Thermal characteristics of a new metal/polymer material for FDM rapid prototyping process," *Assembly Automation*, vol. 25, no. 4, 2005, pp. 309-315

[McMahon 1998] McMahon, C., and Browne, J., *CADCAM principles, practice and manufacturing management, Second Edition*, Addison Wesly Longman Limited, Essex, England, 1998, pp. 88-98

[Meyers 1999] Meyers, M. A., and Chawla, K. K., *Mechanical Behavior of Materials*, Prentice-Hall Inc., New Jersey, USA, 1999, pp. 328-329

[MIT 2005] (Massachusetts Institute of Technology) http://web.mit.edu/tdp/www/whatis3dp.html Downloaded November, 2005

[Noorani 2006] Noorani, R., *Rapid Prototyping: Principles and Applications*, John Wiley & Sons Inc., Hoboken, New Jersey, 2006, pp. 1, 108-125

[Pham 2001] Pham, D. T., and Dimov, S. S., *Rapid Manufacturing: The Technologies and Applications of Rapid Prototyping and Rapid Tooling*, Springer-Verlag London Ltd., London, Great Britain, 2001, pp. 1, 21-23, 161-182

[PML Inc 2005] http://www.pmli.com/equip.html Downloaded November, 2005

[Rodríguez 2001] Rodríguez, J. F., Thomas, J. P., and Renaud, J. E., "Mechanical behavior of acrylonitrile butadiene styrene (ABS) fused deposition materials. Experimental investigation," *Rapid Prototyping Journal*, vol. 7, no. 3, 2001, pp. 148-158

[Rosato 1995] Rosato, D. V., and Rosato, D. V., *Injection Molding Handbook, Second Edition*, Chapman & Hall, New York, USA, 1995, pp. 229-230

[Sabourin 1997] Sabourin, E., Houser, S. A., and Bøhn J. H., "Accurate exterior, fast interior layered manufacturing," *Rapid Prototyping Journal*, vol. 3, no. 2, 1997, pp. 44-52

[Singare 2005] Singare, S., Dichen, L., Bingheng, L., Zhenyu, G., and Yaxiong, L., "Customized design and manufacturing of chin implant based on rapid prototyping," *Rapid Prototyping Journal*, vol. 11, no. 2, 2005, pp. 113-118

[Shofner 2003] Shofner, M. L., Lozano, K., Rodriguez-Macias, F. J., Barrera, E. V., "Nanofiber-reinforced polymers prepared by fused deposition modeling," *Journal of applied polymer science*, vol. 89, no. 11, 2003, pp. 3081-3090

[Stewart 1995] Stewart, J., *Calculus*, Third Edition, Brooks/Cole Publishing Co., California, USA, 1995, pp. 308-313

[Sperling 2006] Sperling, L. H., *INTRODUCTION TO PHYSICAL POLYMER SCIENCE, Fourth Edition*, John Wiley & Sons, Inc., New Jersey, USA, 2006, pp. 2-6

[Stratasys 1997] Stratasys Inc., "QuickSlice Training Manual Release 5.0," Stratasys Document NO: QSTM50, 1997

[Tyberg 1998] Tyberg, J., "Local Adaptive Slicing for Layered Manufacturing," M.S. Thesis, Virginia Polytechnic Institute and State University, Blacksburg, Virginia, USA, 1998

[Vaidyanathan 2000] Vaidyanathan, R., Walish, J., Lombardi, J. L., Kasichainula, S., Calvert, P., and Cooper, K.C., "The Extrusion Freeforming of Functional Ceramic Prototypes," *The Journal of the Minerals, Metals, & Materials Society* (JOM), December 2000, pp. 34-37

[Wang 2004] Wang, J., and Shaw, L., "Rapid Prototyping of Dental Restoration via Multi-Material Slurry Extrusion," *ASM Materials Solutions Conference & Show, Session 4: Rapid Prototyping: Process and Properties II*, Columbus Ohio, October 18, 2004

[Wikipedia 2006] http://en.wikipedia.org
Downloaded August, 2006

[Zhu 2002] Zhu, W. M., and Yu, K. M., "Tool path generation of multi-material assembly for rapid manufacture," *Rapid Prototyping Journal*, vol. 8, no. 5, 2002, pp. 277-283

Curriculum Vitae

John Paul Wachsmuth attended The Ohio State University and pursued a degree in Materials Science Engineering. While in school, John co-oped three times at Thermodisc Inc. (located in Mansfield, OH). There he was introduced to a wide range of engineering roles while working with Positive Temperature Coefficient Thermistors (PTC's). His accomplishments include researching void formation, inventing terminals for inline electrical resistance measurement, and designing/building custom equipment for measuring the resistance of carbon black powder. John also worked part time at Worthington Industries Technical Services as a metallurgical lab technician in order to help pay his tuition. This unassuming position allowed him to become well versed in microstructural analysis, tensile testing, r-bar testing, and other mechanical characterization techniques.

For his Senior Research John examined the stability of Yttrium Oxide in contact with various molten metals for which a ceramic thermistor would be of interest. He graduated in December 2000. After graduating he accepted a position at Materials Modification Inc, a Small Business Innovative Research (SBIR) company located in Fairfax, Virginia. While working there, he submitted proposals, oversaw a multitude of nanoparticle based research contracts, authored publications, trained new employees, increased safety awareness and practices, maintained equipment, and designed the next generation of microwave-plasma based nanoparticle production machines.

In January 2004 John began a Master's Degree in Mechanical Engineering at the Virginia Polytechnic Institute and State University. He completed the required coursework for his degree in 2006 with a 4.0 GPA.